Attacker-Resilient Adaptive Path Following of a Quadrotor with Environment-Aware Dynamic Constraints

Xu Jin, Member, IEEE University of Kentucky, Lexington, KY 40506, USA

Zhongjun Hu

University of Kentucky, Lexington, KY 40506, USA

Abstract— For most works on constrained motion control in the literature, only constant or time-varying constraints are discussed, which are often conservative and cannot adapt to the dynamically changing operation environment. In this work, in the context of quadrotor operations, we propose an adaptive path following architecture with environment-aware dynamic constraints, in which the desired path coordinate, desired path speed, and constraint requirements not only depend on a path parameter associated with the desired path, but also can adapt to the presence of an "attacker" nearby. "Composite barrier function" has been proposed to address both safety and performance constraints in a unified structure. Adaptive laws are introduced to estimate the upper bounds of system uncertainties and unknown "attacker" velocity. Exponential convergence into small neighborhoods around the equilibrium for position and attitude tracking errors can be guaranteed. In the end, a simulation example further demonstrates the effectiveness of the proposed architecture.

Index Terms— Environment-aware dynamic constraints, Composite barrier function, Path-following control, Quadrotor

I. Introduction

Constrained motion control for autonomous vehicles has been rigorously studied in recent years. Constraint requirements can be broadly classified as performance and safety constraints. Violation of such requirements can lead to performance degradation and/or system damages, which can result in mission failures.

Common approaches in handling constraint requirements include model predictive control [1], [2], barrier functions/barrier Lyapunov functions [3], [4], control barrier functions [5], [6], and prescribed performance control [7], [8]. However, almost all existing works on motion

Manuscript received XXXXX 00, 0000; revised XXXXX 00, 0000; accepted XXXXX 00, 0000.

The authors are withthe Department of Mechanical and Aerospace Engineering, University of Kentucky, Lexington, KY 40506, USA (e-mail: xu.jin@uky.edu, ZhongjunHu@uky.edu).

0018-9251 © IEEE

stabilization or trajectory tracking only address constraint requirements that are constant or at best time-varying. Such constraints are often conservative in formulation, as control designers often have to assume worst case scenarios when formulating the constraints. Moreover, constant or time-varying constraints cannot respond well to the operation environment that is varying but not time-dependent.

In view of such limitations, path-following control [9]–[13] is a better alternative in many applications, where the goal is to follow a user-defined spatial path, with no time parameterization. The desired path is dependent on certain path parameters instead of time, hence path-following frameworks can respond better to the environment. Our recent work [14] proposed constrained path-following control architectures, where the constraint requirements depend on a path parameter, instead of being merely constants or time-varying. Such architectures focus on the spatial path following task without temporal restrictions, and hence can result in less aggressive dynamic behavior.

However, all of the aforementioned constraint requirements, either constant, time-varying, or path-dependent, cannot respond well to an external dynamic "attacker" that can be physically present near the autonomous vehicle. This consideration on "attackers" has practical importance in a wide range of applications. For example, when an autonomous drone is conducting a surveillance mission following a pre-planed path, an "attacker" can attempt to fly close to the drone, in order to secretly gather sensitive information, interrupt the communication channel, or simply to collide with the drone in a kamikaze style. In this example, not only the desired path coordinate and desired path speed for the autonomous drone should adapt to the presence of "attacker", but also the constraint requirements should be adjusted depending on the "attacker" state. For instance, if the "attacker" is far away, the constraint requirements can be relaxed in order to avoid excessive control actions; whereas when the "attacker" is closing in, the constraint requirements should be more stringent, in order to ensure the safety and performance of the operation.

In this work we propose the idea of "environmentaware dynamic constraints" in response to an "attacker" operating near an autonomous quadrotor. This "attacker" can adjust its velocity based on the relative distance with respect to the quadrotor, hence it has a certain degree of intelligence. Main technical difficulties come from the new problem formulation, where desired path coordinate, desired path speed, and constraint requirements not only depend on a path parameter associated with the desired path, but also can adapt to the "attacker" nearby. Both safety and performance constraint requirements are addressed, in which the safety constraint prevents the autonomous quadrotor from colliding with the "attacker", and the performance constraint requires the quadrotor to stay close to the desired path. We propose a new concept of "composite barrier function", which is a unified structure to guarantee both safety and performance constraint requirements simultaneously. A path parameter timing law is also integrated with the controller, which serves as a bridge between time-domain system dynamics and path-dependent desired path and constraint requirements. System uncertainties and unknown "attacker" velocity are estimated by adaptive laws. Exponential convergence into small neighborhoods around the equilibrium for position and attitude tracking errors can be guaranteed.

The main novelties and contributions of this paper can be summarized as the following:

- 1. For the first time in the literature, we study a new class of "environment-aware dynamic constraints", which depend on a dynamic path variable and the relative distance with respect to the "attacker". This is in contrast to the existing literature on dynamic obstacles that only consider constant or time-varying constraints [15]–[22], which are conservative and cannot adapt to the dynamically changing environment. More discussion can be see in Section II-C.
- 2. The desired path coordinate and desired path speed in this work are also depending the path variable and the presence of "attacker", giving more abilities to adapt to the dynamically changing environment. More discussion can be seen in Section II-B.
- 3. Unlike many works on obstacle avoidance that only consider obstacles which are static/time-varying [23]–[28] or based on constant velocity assumption [29], [30], in this work we assume the "attacker" velocity is *unknown* and related with the relative position between the quadrotor and "attacker". More discussion can be seen in Section III.
- 4. System uncertainties and disturbances can also be effectively dealt with by the proposed framework.

Compared with out recent works on constrained mobile robot control [14], [31]-[36], this work has the following unique contribution:

- Compared with our recent works [31]-[36], which only consider time-varying constraint requirements on the mobile robot operation, in this work we consider environment-aware dynamic constraints that depend on both a path parameter and an external "attacker". Compared with constant or time-varying constraint requirements, the new formulation on the constraint requirements make the system more adaptable to the dynamically changing operation environment, where the change in environment is not necessarily time dependent.
- 2. Compared with our recent work [14], which addresses path-dependent constraint requirements, in this work we also take the influence of a dynamical "attacker" into the constraint formulation. Moreover, the desired path coordinate and desired path speed also take the "attacker" into consideration, giving the algorithm more degrees of freedom to adapt to the dynamically changing operation environment.

We will use the following standard notations in this paper. First, $\mathbb R$ is real number set and I_m denotes the $m \times m$ identity matrix. Moreover, $(\cdot)^{\mathrm{T}}$ is the transpose of (\cdot) , $|\cdot|$ represents the absolute value for scalars, and $|\cdot|$ represents the Euclidean norm for vectors and induced norm for matrices. Furthermore, we use $c\theta$ to denote $\cos \theta$, $s\theta$ to denote $\sin \theta$, and $t\theta$ to denote $\tan \theta$. We also write (\cdot) as the first order time derivative of (\cdot) , if (\cdot) is differentiable, and $(\cdot)^{(n)}$ as the *n*-th order time derivative of (\cdot) for n being a positive integer. Besides, for any two vectors $v_1, v_2 \in \mathbb{R}^3$, the cross-product operator $\mathbb{S}(\cdot)$ gives $\mathbb{S}(v_1)v_2 = v_1 \times v_2$. It is also true that $\mathbb{S}(v_1)v_2 = -\mathbb{S}(v_2)v_1$ and $v_1^{\mathrm{T}}\mathbb{S}(v_2)v_1=0$. Next, \otimes represents the Kronecker product. In addition, for any matrix $A \in \mathbb{R}^{n \times m}$ where $A = [A_1, \cdots, A_m]$ and $A_j \in \mathbb{R}^n, j = 1, \cdots, m$, the vector operator $\text{vec}(\cdot)$ gives $\text{vec}(A) = [A_1^{\text{T}}, \cdots, A_m^{\text{T}}]^{\text{T}} \in \mathbb{R}^{nm}$. Finally, SO(3) = $\{\Omega \in \mathbb{R}^{3 \times 3} \mid \Omega^{\mathrm{T}} \Omega = I_3\}$ is a set of orthogonal matrices in $\mathbb{R}^{3\times 3}$, and $S^2 = \{x \in \mathbb{R}^3 \mid ||x|| = 1\}$ is a set of unit vectors in \mathbb{R}^3 .

II. Problem formulation

A. System Dynamics

Consider a quadrotor with the following dynamics

$$m\ddot{p}(t) = -F(t)R(\Theta(t))e_z + mge_z + N_1(t), \qquad (1)$$

$$\dot{\Theta}(t) = T(\Theta(t))\omega(t), \tag{2}$$

$$J\dot{\omega}(t) + \mathbb{S}(\omega(t))J\omega(t) = \tau(t) + N_2(t), \tag{3}$$

where $p(0)=p_{10}\in\mathbb{R}^3,\ \dot{p}(0)=p_{20}\in\mathbb{R}^3,\ \Theta(0)=\Theta_0\in\mathbb{R}^3,\ \omega(0)=\omega_0\in\mathbb{R}^3$ are initial conditions. Moreover, $m\in\mathbb{R},\ m>0$ is mass of the quadrotor, and $J\in\mathbb{R}^{3\times3}$ is a symmetric positive definite matrix representing the inertia. The position and attitude in the inertial reference frame are represented as $p(t)=[x(t),\ y(t),\ z(t)]^{\mathrm{T}}\in\mathbb{R}^3$ and $\Theta(t)=[\phi(t),\ \theta(t),\ \psi(t)]^{\mathrm{T}}\in\mathbb{R}^3$, respectively. $F(t)\in\mathbb{R}$ and $\tau(t)\in\mathbb{R}^3$ represent the thrust and torques, respectively. $N_1(t)\in\mathbb{R}^3$ and $N_2(t)\in\mathbb{R}^3$ denote the external disturbances. Furthermore, $g\in\mathbb{R}$ is the gravitational acceleration and $e_z=[0,\ 0,\ 1]^{\mathrm{T}}\in\mathbb{R}^3$ is a unit vector. $R(\Theta(t))\in\mathrm{SO}(3)$ is a rotation matrix, which translates the translational velocity vector in the body-fixed frame into the rate of change of the position vector in the inertial frame

$$R(\Theta) = \begin{bmatrix} c\theta c\psi & s\phi s\theta c\psi - c\phi s\psi & c\phi s\theta c\psi + s\phi s\psi \\ c\theta s\psi & s\phi s\theta s\psi + c\phi c\psi & c\phi s\theta s\psi - s\phi c\psi \\ -s\theta & s\phi c\theta & c\phi c\theta \end{bmatrix}.$$
(4)

Moreover, define a body-fixed frame with the origin being at the center of mass for each quadrotor, and the rotational velocities with respect to this body-fixed frame are denoted by $\omega(t) = [\omega_x(t), \ \omega_y(t), \ \omega_z(t)]^{\mathrm{T}} \in \mathbb{R}^3$. Besides, $T(\Theta(t))$ is a transformation matrix that relates the angular velocity in the body-fixed frame to the rate of change of Euler angles in the inertial frame, and is given

by

$$T(\Theta) = \begin{bmatrix} 1 & s\phi t\theta & c\phi t\theta \\ 0 & c\phi & -s\phi \\ 0 & s\phi/c\theta & c\phi/c\theta \end{bmatrix}.$$
 (5)

As shown in Appendix A (see (48)–(52)), the angular motion dynamics (2) and (3) can be rewritten as

$$M(\Theta(t))\ddot{\Theta}(t) + C(\Theta(t), \dot{\Theta}(t))\dot{\Theta}(t)$$

= $\Psi^{\mathrm{T}}(\Theta(t))J^{\mathrm{T}}\tau(t) + \Psi^{\mathrm{T}}(\Theta(t))J^{\mathrm{T}}N_{2}(t),$ (6)

where $\Psi(\Theta(t))$, $M(\Theta(t))$, and $C(\Theta(t), \dot{\Theta}(t))$ are given in (48), (51), and (52), respectively.

B. Path-Following Problem in the Presence of "Attacker"

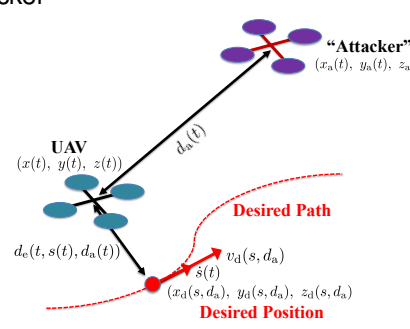


Fig. 1. Path-following in the presence of an "attacker".

See Fig. 1 for an illustration of the path-following problem in the presence of an "attacker". During the path following task, the quadrotor can be interrupted by an "attacker". In this case, define the LOS distance $d_{\rm a}(t)$ between the quadrotor and "attacker" as

$$d_{\rm a}(t) \triangleq \sqrt{(x-x_{\rm a})^2 + (y-y_{\rm a})^2 + (z-z_{\rm a})^2},$$
 (7)

where $p_{\rm a}(t)=[x_{\rm a}(t),\ y_{\rm a}(t),\ z_{\rm a}(t)]^{\rm T}$ is the "attacker" position.

Desired path coordinate for the quadrois denoted by $p_{\rm d}(s(t), d_{\rm a}(t))$ $[x_{\mathbf{d}}(s(t), d_{\mathbf{a}}(t)), y_{\mathbf{d}}(s(t), d_{\mathbf{a}}(t)), z_{\mathbf{d}}(s(t), d_{\mathbf{a}}(t))]^{\mathrm{T}} \in \mathbb{R}^{3},$ where $s(t) \in \mathbb{R}$ is a path parameter and $p_{\rm d}(s(t), d_{\rm a}(t))$ is at least three-times continuously differentiable and have bounded derivatives with respect to s(t) and $d_a(t)$. Note that in Fig. 1, $p_d(s(t), d_a(t))$ is not necessarily the vehicle's closest/projection point on the desired path. Finally, $v_{\rm d}(s(t), d_{\rm a}(t))$ is the desired path speed associated with the path parameter s(t) and "attacker" distance $d_{\rm a}(t)$.

Remark 2.1:

Note that the desired path $p_{\rm d}(s(t),d_{\rm a}(t))$ is dependent on the "attacker" distance $d_{\rm a}(t)$. That is, the desired path can be modified according to the relative distance between the quadrotor and "attacker". This dependence gives an additional degree of freedom for the desired path to be adjusted in the presence of "attacker". This is also the case for the desired path speed $v_{\rm d}(s(t),d_{\rm a}(t))$.

C. System Safety and Performance Constraints

During the path following problem defined in the aforementioned subsection B, certain system constraint requirements that need to be satisfied, in order to ensure *safe* and *precise* operation. First, to ensure safe operation, the quadrotor needs to avoid collision with the "attacker" at all time. Namely, the quadrotor needs to satisfy the following *safety constraint*

$$d_{\mathbf{a}}(t) > \Omega_{\mathbf{a}}(s(t)), \tag{8}$$

where $\Omega_{\rm a}(s(t))>0$ is a user-defined path-dependent constraint requirement, which is designed to be at least three-times continuously differentiable and has bounded derivatives with respect to s(t). Moreover, $\Omega_{\rm a}(s(t))$ is designed such that when $t=0,\ d_{\rm a}(0)>\Omega_{\rm a}(s(0))$.

Second, the LOS distance tracking error $d_{\rm e}(t,s(t),d_{\rm a}(t))$, the distance between the quadrotor's actual and desired positions, is

$$d_{\rm e} \triangleq \sqrt{(x - x_{\rm d})^2 + (y - y_{\rm d})^2 + (z - z_{\rm d})^2}.$$
 (9)

To ensure precise path following, and also to adapt to the "attacker" nearby, the following *performance constraint* needs to be guaranteed

$$d_{\rm e}(t, s(t), d_{\rm a}(t)) < \Omega_{\rm H}(s(t), d_{\rm a}(t)),$$
 (10)

where $\Omega_{\rm H}(s(t),d_{\rm a}(t))>0$ is the user-defined path-dependent constraint requirement for the distance tracking error that can also respond to the changing LOS distance between the quadrotor and "attacker". Note that $\Omega_{\rm H}(s(t),d_{\rm a}(t))$ is designed to be at least three-times continuously differentiable and has bounded derivatives with respect to s(t) and $d_{\rm a}(t)$. Moreover, $\Omega_{\rm H}(s(t),d_{\rm a}(t))$ is designed such that when $t=0,\ d_{\rm e}(0,s(0),d_{\rm a}(0))<\Omega_{\rm H}(s(0),d_{\rm a}(0))$.

It is easy to see from (9) that $d_{\rm e}(t,s(t),d_{\rm a}(t))\geq 0$ at all time. However, in order to avoid singularity in the controller design, it is needed for $d_{\rm e}(t,s(t),d_{\rm a}(t))$ to be bounded away from the origin. Therefore, the constraint requirement (10) is modified as

$$0 < \varepsilon < d_{\mathbf{e}}(t, s(t), d_{\mathbf{a}}(t)) < \Omega_{\mathbf{H}}(s(t), d_{\mathbf{a}}(t)), \tag{11}$$

where ε is an user-defined positive number that can be arbitrarily small. Note that (11) is equivalent to

$$-\varepsilon < d_{e2}(t, s(t), d_{a}(t)) < \Omega_{H2}(s(t), d_{a}(t)),$$
 (12)

where $d_{\rm e2}(t,s(t),d_{\rm a}(t)) \triangleq d_{\rm e}(t,s(t),d_{\rm a}(t)) - 2\varepsilon$ and $\Omega_{\rm H2}(s(t),d_{\rm a}(t)) \triangleq \Omega_{\rm H}(s(t),d_{\rm a}(t)) - 2\varepsilon$. More discussion on how the modified constraint requirement (12) can help avoid singularity in the control design can be seen in the later Remark 5.1.

Last but not least, define the attitude tracking error as

$$z_{\Theta}(t) = [z_{\phi}(t), z_{\theta}(t), z_{\psi}(t)]^{\mathrm{T}} = \Theta(t) - \Theta_{\mathrm{d}}(t), \quad (13)$$

where $\Theta_{\rm d}(t) = [\phi_{\rm d}(t), \; \theta_{\rm d}(t), \; \psi_{\rm d}(t)]^{\rm T} \in \mathbb{R}^3$ is the desired attitude to be specified later.

3

D. Control Objective

The **control objective** for the path-following problem is to design a control framework such that:

- 1) The modified tracking error $d_{\rm e2}(t,s(t),d_{\rm a}(t))$ for the quadrotor can converge into an arbitrarily small region around the equilibrium. Equivalently, this means the LOS distance tracking error $d_{\rm e}(t,s(t),d_{\rm a}(t))$ can converge into an arbitrarily small region around 2ε , where $\varepsilon>0$ is an arbitrarily small constant;
- 2) The attitude tracking error $z_{\Theta}(t) = [z_{\phi}(t), z_{\theta}(t), z_{\psi}(t)]^{T}$ can converge into an arbitrarily small neighborhood of zero;
- 3) The quadrotor satisfies a desired speed assignment $v_{\rm d}(s(t),d_{\rm a}(t))\in\mathbb{R}$, which is at least twice continuously differentiable and has bounded derivatives with respect to s(t) and $d_{\rm a}(t)$. That is, $z_s(t)=\dot{s}(t)-v_{\rm d}(s(t),d_{\rm a}(t))$ can converge into an arbitrarily small neighborhood of zero:
- 4) The safety and performance constraints (8) and (12) will not be violated during formation.

We will need the following assumptions for the analysis and discussion of our main theoretical results.

Assumption 2.1:

The "attacker" is "avoidable", which is defined as the unit vector between the quadrotor and desired path not being in the same line as the unit vector between the quadrotor and "attacker".

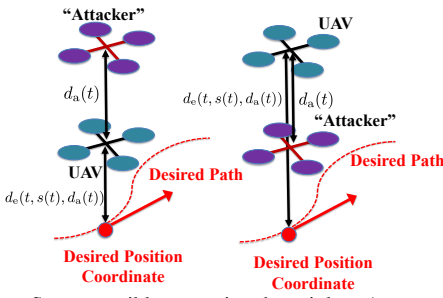


Fig. 2. Some possible scenarios that violate Assumption 2.1.

Remark 2.2:

See Fig. 2 for some of the possible scenarios that violate Assumption 2.1. Essentially, Assumption 2.1 means that the desired path coordinate $p_{\rm d}(s(t),d_{\rm a}(t))$, the quadrotor position p(t), and the "attacker" position $p_{\rm a}(t)$ cannot be on the same line. Note that the desired path coordinate $p_{\rm d}(s(t),d_{\rm a}(t))$, desired path speed $v_{\rm d}(s(t),d_{\rm a}(t))$, and performance constraint $\Omega_{\rm H2}(s(t),d_{\rm a}(t))$ all depend on the LOS distance $d_{\rm a}(t)$ between the quadrotor and "attacker", which is a scalar without a direction. Therefore, both scenarios in Fig. 2 violate the "avoidability" assumption. More discussion on "avoidability" can be seen in Remark 5.1.

Remark 2.3:

It is worth pointing out that Assumption 2.1 is not restrictive. Note that the desired path coordinate $p_{\rm d}(s(t),d_{\rm a}(t))$ can depend both on the path parameter s(t) and the LOS

"attacker" distance $d_{\rm a}(t)$. That is, the desired path coordinate has two degrees of freedom in design. Therefore it is relatively easy to modify the desired path coordinate to satisfy this "avoidablility" assumption.

Assumption 2.2:

The desired path coordinate $p_{\rm d}(s(t),d_{\rm a}(t))$ is at least three-times continuously differentiable and have bounded derivatives with respect to s(t) and $d_{\rm a}(t)$. Furthermore, for the reference attitude we assume $\phi_{\rm d}(t) \in (-\frac{\pi}{2}, \frac{\pi}{2})$, $\theta_{\rm d}(t) \in (-\frac{\pi}{2}, \frac{\pi}{2})$, and $\psi_{\rm d}(t) \in [-\pi, \pi]$, where $\psi_{\rm d}(t)$ is at least twice continuously differentiable and has bounded derivatives with respect to time.

Assumption 2.3 ([37], [38]):

The thrust F(t) and external disturbances $N_1(t)$ and $N_2(t)$ for the quadrotor are uniformly bounded with unknown bounds.

Assumption 2.4:

The "attacker" velocity is continuous and related with the relative position between the quadrotor and "attacker", that is, the "attacker" velocity can be expressed as $v_{\rm a}(Z_{\rm a})$ with $Z_{\rm a}=[x-x_{\rm a},\ y-y_{\rm a},\ z-z_{\rm a}]^{\rm T}\in\mathbb{R}^3$. Furthermore, the "attacker" velocity $v_{\rm a}(Z_{\rm a})$ is unknown.

Remark 2.4:

According to Assumption 2.4, the physical attacker is assumed to possess a certain level of intelligence. As a result, the physical attacker problem examined in this study cannot be effectively resolved using conventional obstacle-avoidance mechanisms that solely account for static or time-varying obstacles.

Assumption 2.5 ([37]):

The mass m of the quadrotor can be measured. However, the inertia J is $\underline{\mathit{unknown}}$ and is assumed to be bounded, such that for any $z \in \mathbb{R}^3$, $\underline{\mathit{J}}z^{\mathrm{T}}z \leq z^{\mathrm{T}}\mathit{Jz} \leq \bar{\mathit{J}}z^{\mathrm{T}}z$, where $\bar{\mathit{J}}$ and $\underline{\mathit{J}}$ are $\underline{\mathit{unknown}}$ positive constants. As a direct result, the symmetric positive definite matrix $M(\Theta)$ in (51) is also $\underline{\mathit{unknown}}$ and bounded, such that for any $z \in \mathbb{R}^3$, $\underline{\mathit{M}}z^{\mathrm{T}}z \leq z^{\mathrm{T}}M(\Theta)z \leq \bar{\mathit{M}}z^{\mathrm{T}}z$, where $\bar{\mathit{M}}$ and $\underline{\mathit{M}}$ are $\underline{\mathit{unknown}}$ positive constants.

Assumption 2.6 ([38]):

The attitude of the quadrotor is confined such that $\phi \in (-\frac{\pi}{2}, \frac{\pi}{2})$, $\theta \in (-\frac{\pi}{2} + \varepsilon_{\theta}, \frac{\pi}{2} - \varepsilon_{\theta})$ and $\psi \in [-\pi, \pi]$ for some $\varepsilon_{\theta} > 0$. The boundedness of ϕ and θ guarantees that $T(\Theta)$ is invertible during the operation.

The following lemmas are needed for the controller design and theoretical analysis to be presented.

Lemma 2.1 ([39]):

For any constant $\epsilon>0$ and any variable $z\in\mathbb{R}$, we have $0\leq |z|-\frac{z^2}{\sqrt{z^2+\epsilon^2}}<\epsilon.$

Lemma 2.2 ([40]):

Let $A \in \mathbb{R}^{n \times m}$, $B \in \mathbb{R}^{m \times l}$, and $C \in \mathbb{R}^{l \times k}$. Then $vec(ABC) = (C^T \otimes A)vec(B)$.

III. Radical Basis Function Neural Networks

In our formation control design, radical basis function neural networks (RBFNNs) [41]–[43] will be utilized to estimate the unknown attacker velocity $v_{\rm a}(Z_{\rm a}):\mathbb{R}^3\to\mathbb{R}^3$. Specifically, for a continuous nonlinear function $v_{\rm a}(Z_{\rm a})$ defined over a compact set $\Omega_{Z{\rm a}}\subset\mathbb{R}^3$, there exist RBFNNs $W_{\rm a}^{\rm T}B_{\rm a}(Z_{\rm a})$ given as

$$v_{\mathbf{a}}(Z_{\mathbf{a}}) = W_{\mathbf{a}}^{\mathrm{T}} B_{\mathbf{a}}(Z_{\mathbf{a}}) + \delta_{\mathbf{a}}(Z_{\mathbf{a}}),$$

where $Z_{\rm a}\in\Omega_{Z{\rm a}}\subset\mathbb{R}^3$ is the input vector, $W_{\rm a}=[w_{\rm a1},\cdots,w_{\rm an}]^{\rm T}\in\mathbb{R}^{n\times 3}$ where $w_{\rm ak}=[w_{\rm ak1},\ w_{\rm ak2},\ w_{\rm ak3}]^{\rm T}\in\mathbb{R}^3\ (k=1,\cdots,n),\ n\geq 1$ is the number of neural network node, $B_{\rm a}(Z_{\rm a})=[b_1(Z_{\rm a}),\cdots,b_n(Z_{\rm a})]^{\rm T}\in\mathbb{R}^n$ is the basis function vector, and $\delta_{\rm a}(Z_{\rm a})=[\delta_{\rm a1}(Z_{\rm a}),\ \delta_{\rm a2}(Z_{\rm a}),\ \delta_{\rm a3}(Z_{\rm a})]^{\rm T}\in\mathbb{R}^3$ is the approximation error satisfying $||\delta_{\rm a}(Z_{\rm a})||\leq \bar{\delta}_{\rm a}$, where $\bar{\delta}_{\rm a}>0$ is a given precision level. The basis function $b_k(Z_{\rm a})$ is usually selected as the following Gaussian-like function

$$b_k(Z_{\mathbf{a}}) = \exp \left[-\frac{(Z_{\mathbf{a}} - \nu_k)^{\mathrm{T}}(Z_{\mathbf{a}} - \nu_k)}{\zeta_k^2} \right],$$

with $\nu_k = [\nu_{k1}, \ \nu_{k1}, \ \nu_{k3}]^{\mathrm{T}} \in \mathbb{R}^3$ being the receptive field's center and $\zeta_k \in \mathbb{R}$ being the width of the Gaussian-like function $b_k(Z_{\mathrm{a}}), \ k=1,\cdots,n$. Moreover, $W_{\mathrm{a}} = [w_{\mathrm{a}1},\cdots,w_{\mathrm{a}n}]^{\mathrm{T}} \in \mathbb{R}^{n \times 3}$ is an ideal weight matrix defined as

$$W_{\mathbf{a}} := \arg\min_{\hat{W}_{\mathbf{a}} \in \mathbb{R}^{n \times 3}} \Bigg\{ \sup_{Z_{\mathbf{a}} \in \Omega_{Z_{\mathbf{a}}}} \bigg| \bigg| v_{\mathbf{a}}(Z_{\mathbf{a}}) - \hat{W}_{\mathbf{a}}^{\mathsf{T}} B_{\mathbf{a}}(Z_{\mathbf{a}}) \bigg| \bigg| \Bigg\},$$

where $\hat{W}_{a} \in \mathbb{R}^{n \times 3}$ denotes the weight matrix.

IV. Composite Barrier Function

In this section, we introduce the concept of "composite barrier function" to address environment-aware dynamic constraint requirements. Specifically, taking constraint requirements (8) and (12) into considerations, we first introduce the following transformed error variables

$$\eta_{\rm e} = \frac{\Omega_{\rm H2} d_{\rm e2}}{(\Omega_{\rm H2} - d_{\rm e2})(\varepsilon + d_{\rm e2})}, \quad \eta_{\rm a} = \frac{1}{d_{\rm a} - \Omega_{\rm a}}.$$
(14)

Note that $\eta_{\rm e}=0$ only when $d_{\rm e2}=0$ and $\eta_{\rm a}=0$ only when $d_{\rm a}\to\infty$. The "composite barrier function" to deal with the constraint requirements (8) and (12) is then designed as

$$V_p = \frac{1}{2}\eta_{\rm e}^2 + \frac{1}{2}\eta_{\rm a}^2. \tag{15}$$

Remark 4.1:

The function (15) is called "composite barrier function", since it takes both safety and performance constraint requirements into consideration. Note that the safety and performance constraints are on different distance tracking variables. On the one hand, when the safety constraint

(8) is to become violated, we will have $d_{\rm a} \to \Omega_{\rm a}$, and hence $\eta_{\rm a} \to \infty$. On the other hand, when the performance constraint (12) is to become violated, we get $d_{\rm e2} \to \Omega_{\rm H2}$ or $d_{\rm e2} \to -\varepsilon$, and hence $\eta_{\rm e} \to \infty$. Therefore, by keeping the "composite barrier function" uniformly bounded through closed-loop analysis, we can ensure that both safety and performance constraint requirements will be satisfied during the operation.

To simplify the discussion and analysis to be presented, we will omit the variables' dependence on time, state, and path parameters when there is no potential for any confusion.

V. Control Design and Main Results

Here we present the controller design procedure based on backstepping, which will lead to our main theoretical results.

A. Distance Control Design and Results

Step 1:

We first consider the time derivative of the "composite barrier function" (15), which leads to

$$\dot{V}_{p} = \eta_{e} \frac{\partial \eta_{e}}{\partial \Omega_{H2}} \left(\frac{\partial \Omega_{H2}}{\partial s} \dot{s} + \frac{\partial \Omega_{H2}}{\partial d_{a}} \frac{1}{d_{a}} E_{a}^{T} (\dot{p} - \dot{p}_{a}) \right)
+ \eta_{e} \frac{\partial \eta_{e}}{\partial d_{e2}} \frac{1}{d_{e}} E_{d}^{T} \left(\dot{p} - \frac{\partial p_{d}}{\partial s} \dot{s} - \frac{\partial p_{d}}{\partial d_{a}} \frac{1}{d_{a}} E_{a}^{T} (\dot{p} - \dot{p}_{a}) \right)
+ \eta_{a} \frac{\partial \eta_{a}}{\partial d_{a}} \frac{1}{d_{a}} E_{a}^{T} (\dot{p} - \dot{p}_{a}) + \eta_{a} \frac{\partial \eta_{a}}{\partial \Omega_{a}} \frac{d\Omega_{a}}{ds} \dot{s}
= g_{s} \dot{s} + G_{2}^{T} \dot{p} - G_{1}^{T} \dot{p}_{a},$$
(16)

where $E_{\rm a}=[x-x_{\rm a},\ y-y_{\rm a},\ z-z_{\rm a}]^{\rm T}\in\mathbb{R}^3$ and $E_{\rm d}=[x-x_{\rm d},\ y-y_{\rm d},\ z-z_{\rm d}]^{\rm T}\in\mathbb{R}^3$. Furthermore,

$$\begin{split} g_s &= \eta_{\rm e} \frac{\partial \eta_{\rm e}}{\partial \Omega_{\rm H2}} \frac{\partial \Omega_{\rm H2}}{\partial s} - \eta_{\rm e} \frac{\partial \eta_{\rm e}}{\partial d_{\rm e2}} \frac{1}{d_{\rm e}} E_{\rm d}^{\rm T} \frac{\partial p_{\rm d}}{\partial s} + \eta_{\rm a} \frac{\partial \eta_{\rm e}}{\partial \Omega_{\rm a}} \frac{\mathrm{d}\Omega_{\rm a}}{\mathrm{d}s}, \\ g_s &\in \mathbb{R}, \end{split}$$

$$\begin{split} G_{1} &= \left(\eta_{\mathrm{e}} \frac{\partial \eta_{\mathrm{e}}}{\partial \Omega_{\mathrm{H2}}} \frac{\partial \Omega_{\mathrm{H2}}}{\partial d_{\mathrm{a}}} - \eta_{\mathrm{e}} \frac{\partial \eta_{\mathrm{e}}}{\partial d_{\mathrm{e2}}} \frac{1}{d_{\mathrm{e}}} E_{\mathrm{d}}^{\mathrm{T}} \frac{\partial p_{\mathrm{d}}}{\partial d_{\mathrm{a}}} \right. \\ &+ \eta_{\mathrm{a}} \frac{\partial \eta_{\mathrm{e}}}{\partial d_{\mathrm{a}}} \right) \frac{1}{d_{\mathrm{a}}} E_{\mathrm{a}}, \end{split}$$

 $G_2 = G_1 + \eta_e \frac{\partial \eta_e}{\partial d_{e2}} \frac{1}{d_e} E_d, \quad G_1, G_2 \in \mathbb{R}^3.$

Define the fictitious velocity tracking error $z_v = \dot{p} - \alpha_v$, where α_v is a stablizing function to be designed shortly. Moreover, recall from Control Objective 3 that the path speed error is defined as $z_s = \dot{s} - v_{\rm d}$. Now, from (16) we can further have

$$\dot{V}_p = g_s z_s + g_s v_d + G_2^T z_v + G_2^T \alpha_v - G_1^T \dot{p}_a, \tag{17}$$

where, by using Lemmas 2.1 and 2.2, the expression for the term $-G_1^T \dot{p}_a$ can be derived as follows

$$\begin{aligned} -G_{1}^{\mathrm{T}}\dot{p}_{\mathrm{a}} &= -G_{1}^{\mathrm{T}}v_{\mathrm{a}} = -G_{1}^{\mathrm{T}}\left(W_{\mathrm{a}}^{\mathrm{T}}B_{\mathrm{a}} + \delta_{\mathrm{a}}\right) \\ &= -G_{1}^{\mathrm{T}}\left(\hat{W}_{\mathrm{a}}^{\mathrm{T}} - \tilde{W}_{\mathrm{a}}^{\mathrm{T}}\right)B_{\mathrm{a}} - G_{1}^{\mathrm{T}}\delta_{\mathrm{a}} \\ &= -\left(G_{1} \otimes B_{\mathrm{a}}\right)^{\mathrm{T}}\hat{w}_{\mathrm{a}} + \left(G_{1} \otimes B_{\mathrm{a}}\right)^{\mathrm{T}}\tilde{w}_{\mathrm{a}} - G_{1}^{\mathrm{T}}\delta_{\mathrm{a}} \end{aligned}$$

$$< -(G_1 \otimes B_{\mathbf{a}})^{\mathrm{T}} \hat{w}_{\mathbf{a}} + (G_1 \otimes B_{\mathbf{a}})^{\mathrm{T}} \tilde{w}_{\mathbf{a}} \\ + \bar{\delta}_{\mathbf{a}} \frac{||G_1||^2}{\sqrt{||G_1||^2 + \epsilon^2}} + \bar{\delta}_{\mathbf{a}} \epsilon$$

where $\tilde{W}_{\rm a} = \hat{W}_{\rm a} - W_{\rm a}$, $\hat{W}_{\rm a} \in \mathbb{R}^{n \times 3}$ is the estimation of $W_{\rm a}$ by the quadrotor, $\hat{w}_{\rm a} = {\rm vec}(\hat{W}_{\rm a}^{\rm T}) \in \mathbb{R}^{3n}$, $w_{\rm a} = {\rm vec}(W_{\rm a}^{\rm T}) \in \mathbb{R}^{3n}$, and $\tilde{w}_{\rm a} = {\rm vec}(\tilde{W}_{\rm a}^{\rm T}) \in \mathbb{R}^{3n}$. Besides, $\epsilon > 0$ is an arbitrarily small number introduced in view of Lemma 2.1. Next, define the stabilizing function as

$$\alpha_{v} = \frac{G_{2}}{G_{2}^{T}G_{2}} \left(-K_{e}\eta_{e}^{2} - K_{a}\eta_{a}^{2} - g_{s}v_{d} + (G_{1} \otimes B_{a})^{T}\hat{w}_{a} - \hat{\delta}_{a} \frac{||G_{1}||^{2}}{\sqrt{||G_{1}||^{2} + \epsilon^{2}}} \right),$$
(18)

where $K_{\rm e}>0$ and $K_{\rm a}>0$ are control gains, and $\hat{\delta}_{\rm a}$ is an estimator of $\bar{\delta}_{\rm a}$.

Remark 5.1:

In (18), singularity can only happen when $d_{\rm a}=0$, $d_{\rm e}=0$, or $G_2=0$ ($d_{\rm a}\neq 0$ and $d_{\rm e}\neq 0$). However, in view of the safety and performance constraint requirements (8) and (12), we have $d_{\rm a}>\Omega_{\rm a}>0$ and $d_{\rm e}>\varepsilon>0$, hence $d_{\rm a}=0$ and $d_{\rm e}=0$ will not happen if (8) and (12) are satisfied. When $G_2=0$ ($d_{\rm a}\neq 0$ and $d_{\rm e}\neq 0$), recall from (16) that we have

$$\left(\eta_{e} \frac{\partial \eta_{e}}{\partial \Omega_{H2}} \frac{\partial \Omega_{H2}}{\partial d_{a}} - \eta_{e} \frac{\partial \eta_{e}}{\partial d_{e2}} \frac{1}{d_{e}} E_{d}^{T} \frac{\partial p_{d}}{\partial d_{a}} + \eta_{a} \frac{\partial \eta_{e}}{\partial d_{a}}\right) \frac{1}{d_{a}} E_{a}$$

$$= -\eta_{e} \frac{\partial \eta_{e}}{\partial d_{e2}} \frac{1}{d_{e}} E_{d}, \tag{19}$$

which means that the unit vector between the quadrotor and "attacker" $\frac{1}{d_a}E_a\in S^2$ is linearly dependent on the unit vector between the quadrotor and desired path coordinate $\frac{1}{d_e}E_d\in S^2.$ Under Assumption 2.1, (19) will never occur. Therefore, singularity will not occur in the stabilizing function design (18).

Hence, denote $\tilde{\delta}_{\rm a}=\hat{\delta}_{\rm a}-\bar{\delta}_{\rm a}$, (17) yields

$$\dot{V}_{p} < -K_{e}\eta_{e}^{2} - K_{a}\eta_{a}^{2} - \tilde{\delta}_{a} \frac{||G_{1}||^{2}}{\sqrt{||G_{1}||^{2} + \epsilon^{2}}}
+ \tilde{w}_{a}^{T}(G_{1} \otimes B_{a}) + g_{s}z_{s} + G_{2}^{T}z_{v} + \bar{\delta}_{a}\epsilon.$$
(20)

Step 2:

At this step, we consider the translational dynamics of the quadrotors. Define $V_v = \frac{1}{2} z_v^{\mathrm{T}} z_v$, and its time derivative gives

$$\dot{V}_{v} = z_{v}^{\mathrm{T}} \left(g e_{z} - \frac{1}{m} u - \frac{1}{m} F(R - R_{\mathrm{d}}) e_{z} + \frac{1}{m} N_{1} - \dot{\alpha}_{v} \right), \tag{21}$$

in which we denote $u = FR_{\mathrm{d}}e_z \in \mathbb{R}^3$ and

$$\dot{\alpha}_{v} = h_{s}\dot{s} + H_{p}\dot{p} - H_{a}\dot{p}_{a} + \frac{\partial\alpha_{v}}{\partial\hat{w}_{a}}\dot{\hat{w}}_{a} + \frac{\partial\alpha_{v}}{\partial\hat{\delta}_{a}}\dot{\hat{\delta}}_{a}, \quad (22)$$

where $h_s \in \mathbb{R}^3$, $H_p \in \mathbb{R}^{3\times 3}$, and $H_a \in \mathbb{R}^{3\times 3}$ are given in Appendix B (see (53)–(55)). Now, the control law $u \in \mathbb{R}^3$ is designed as

$$u = m\bar{u},$$

$$\bar{u} = K_v z_v + G_2 - h_s v_d - H_p^T \dot{p} - \frac{\partial \alpha_v}{\partial \hat{w}_a} \dot{\hat{w}}_a - \frac{\partial \alpha_v}{\partial \hat{\delta}_a} \dot{\hat{\delta}}_a$$

$$+ \hat{\delta}_a \frac{H_a H_a^T z_v}{\sqrt{||H_a^T z_v||^2 + \epsilon^2}} + \hat{\mu}_m \frac{z_v}{\sqrt{||z_v||^2 + \epsilon^2}}$$

$$+ q e_z + (B_z^T \otimes H_a) \hat{w}_a,$$
(24)

where $K_v>0$ is a control gain and $\hat{\mu}_m$ is an estimator of the unknown constant $\bar{\mu}_m$ satisfying $\left|\left|-\frac{1}{m}F(R-R_{\rm d})e_z+\frac{1}{m}N_1\right|\right|\leq\bar{\mu}_m$.

$$\begin{split} \left|\left|-\frac{1}{m}F(R-R_{\rm d})e_z+\frac{1}{m}N_1\right|\right| &\leq \bar{\mu}_m. \\ \text{Hence, denote } \tilde{\mu}_m=\hat{\mu}_m-\bar{\mu}_m, \text{ (20) and (21) lead to} \\ \dot{V}_p+\dot{V}_v \end{split}$$

$$< -K_{e}\eta_{e}^{2} - K_{a}\eta_{a}^{2} - K_{v}z_{v}^{T}z_{v} + \left(g_{s} - z_{v}^{T}h_{s}\right)z_{s}$$

$$-\tilde{\delta}_{a}\left(\frac{||G_{1}||^{2}}{\sqrt{||G_{1}||^{2} + \epsilon^{2}}} + \frac{||H_{a}^{T}z_{v}||^{2}}{\sqrt{||H_{a}^{T}z_{v}||^{2} + \epsilon^{2}}}\right)$$

$$-\tilde{w}_{a}^{T}\left(-(G_{1} \otimes B_{a}) + (H_{a}^{T} \otimes B_{a})z_{v}\right)$$

$$-\tilde{\mu}_{m}\frac{||z_{v}||^{2}}{\sqrt{||z_{v}||^{2} + \epsilon^{2}}} + (2\bar{\delta}_{a} + \bar{\mu}_{m})\epsilon. \tag{25}$$

Next, define $V_s = \frac{1}{2}z_s^2$, its time derivative leads to

$$\dot{V}_s = z_s \dot{z}_s = z_s \left(\ddot{s} - \frac{\partial v_d}{\partial s} \dot{s} - \frac{\partial v_d}{\partial d_a} \frac{1}{d_a} E_a^T (\dot{p} - \dot{p}_a) \right). \tag{26}$$

Now, design the path parameter timing law \ddot{s} as

$$\ddot{s} = -K_s z_s + \frac{\partial v_{\rm d}}{\partial s} \dot{s} + \frac{\partial v_{\rm d}}{\partial d_{\rm a}} \frac{1}{d_{\rm a}} E_{\rm a}^{\rm T} \dot{p} - g_s + z_v^{\rm T} h_s - \frac{\partial v_{\rm d}}{\partial d_{\rm a}} \left(\left(\frac{1}{d_{\rm a}} E_{\rm a} \right) \otimes B_{\rm a} \right)^{\rm T} \hat{w}_{\rm a} - \hat{\delta}_{\rm a} \frac{z_s \left(\frac{\partial v_{\rm d}}{\partial d_{\rm a}} \right)^2}{\sqrt{z_s^2 \left(\frac{\partial v_{\rm d}}{\partial d_{\rm a}} \right)^2 + \epsilon^2}},$$
(27)

where $s(0) = s_{10}$ and $\dot{s}(0) = s_{20}$ are initial conditions, and $K_s > 0$ is a control constant. Therefore,

$$\dot{V}_{p} + \dot{V}_{v} + \dot{V}_{s}
< -K_{e}\eta_{e}^{2} - K_{a}\eta_{a}^{2} - K_{v}z_{v}^{T}z_{v} - K_{s}z_{s}^{2}
- \tilde{\delta}_{a} \left(\frac{||G_{1}||^{2}}{\sqrt{||G_{1}||^{2} + \epsilon^{2}}} + \frac{||H_{a}^{T}z_{v}||^{2}}{\sqrt{||H_{a}^{T}z_{v}||^{2} + \epsilon^{2}}} + \frac{z_{s}^{2}\left(\frac{\partial v_{d}}{\partial d_{a}}\right)^{2}}{\sqrt{z_{s}^{2}\left(\frac{\partial v_{d}}{\partial d_{a}}\right)^{2} + \epsilon^{2}}}\right)
- \tilde{w}_{a}^{T} \left(-(G_{1} \otimes B_{a}) + (H_{a}^{T} \otimes B_{a})z_{v} + z_{s}\frac{\partial v_{d}}{\partial d_{a}}\left(\left(\frac{1}{d_{a}}E_{a}\right) \otimes B_{a}\right)\right)
- \tilde{\mu}_{m}\frac{||z_{v}||^{2}}{\sqrt{||z_{v}||^{2} + \epsilon^{2}}} + (3\bar{\delta}_{a} + \bar{\mu}_{m})\epsilon. \tag{28}$$

Finally, design the adaptive laws as the following

$$\dot{\hat{\delta}}_{a} = n_{\delta a} \left(\frac{||G_{1}||^{2}}{\sqrt{||G_{1}||^{2} + \epsilon^{2}}} + \frac{||H_{a}^{T} z_{v}||^{2}}{\sqrt{||H_{a}^{T} z_{v}||^{2} + \epsilon^{2}}} + \frac{z_{s}^{2} \left(\frac{\partial v_{d}}{\partial d_{a}}\right)^{2}}{\sqrt{z_{s}^{2} \left(\frac{\partial v_{d}}{\partial d_{e}}\right)^{2} + \epsilon^{2}}} \right) - \sigma_{\delta a} \hat{\delta}_{a}, \tag{29}$$

$$\dot{\hat{w}}_{a} = n_{wa} \left(- (G_{1} \otimes B_{a}) + (H_{a}^{T} \otimes B_{a}) z_{v} + z_{s} \frac{\partial v_{d}}{\partial d_{a}} \left(\left(\frac{1}{d_{a}} E_{a} \right) \otimes B_{a} \right) \right) - \sigma_{wa} \hat{w}_{a},$$
(30)

$$\dot{\hat{\mu}}_{m} = n_{\mu m} \frac{||z_{v}||^{2}}{\sqrt{||z_{v}||^{2} + \epsilon^{2}}} - \sigma_{\mu m} \hat{\mu}_{m}, \tag{31}$$

where $\hat{\delta}_{\rm a}(0) = \hat{\delta}_{\rm a0}$, $\hat{w}_{\rm a}(0) = \hat{w}_{\rm a0}$, and $\hat{\mu}_{m}(0) = \hat{\mu}_{m0}$ are initial conditions. $n_{\delta \rm a}$, $\sigma_{\delta \rm a}$, $n_{w \rm a}$, $\sigma_{w \rm a}$, $n_{\mu m}$, and $\sigma_{\mu m}$ are positive design constants.

Design the Lyapunov function candidates for the estimators as $V_{\delta \rm a}=\frac{1}{2n_{\rm sa}}\tilde{\delta}_{\rm a}^2,~V_{w\rm a}=\frac{1}{2n_{\rm wa}}\tilde{w}_{\rm a}^{\rm T}\tilde{w}_{\rm a},$ and $V_{\mu m}=\frac{1}{2n_{\mu m}}\tilde{\mu}_{m}^{2}.$ Now, denote $V_{\rm pos}=V_{p}+V_{v}+V_{s}+V_{\delta \rm a}+V_{w\rm a}+V_{\mu m},$ for its time derivative we can get

$$\dot{V}_{\text{pos}} < -K_{\text{e}} \eta_{\text{e}}^{2} - K_{\text{a}} \eta_{\text{a}}^{2} - K_{v} z_{v}^{\text{T}} z_{v} - K_{s} z_{s}^{2} - \frac{\sigma_{\delta \text{a}}}{2n_{\delta \text{a}}} \tilde{\delta}_{\text{a}}^{2} - \frac{\sigma_{\omega \text{a}}}{2n_{\omega \text{a}}} \tilde{\omega}_{\text{a}}^{\text{T}} \tilde{\omega}_{\text{a}} - \frac{\sigma_{\mu m}}{2n_{\mu m}} \tilde{\mu}_{m}^{2} + \varrho_{1},$$
(32)

where $\varrho_1 = \frac{\sigma_{\delta a}}{2n_{\delta a}}\bar{\delta}_a^2 + \frac{\sigma_{wa}}{2n_{wa}}w_a^Tw_a + \frac{\sigma_{\mu m}}{2n_{\mu m}}\bar{\mu}_m^2 + (3\bar{\delta}_a + \bar{\mu}_m)\epsilon$ is a constant term that can be adjusted. Hence,

$$\dot{V}_{\rm pos} < -\kappa_1 V_{\rm pos} + \varrho_1,\tag{33}$$

where $\kappa_1 \triangleq \min(2K_e, 2K_a, 2K_v, 2K_s, \sigma_{\delta a}, \sigma_{wa}, \sigma_{\mu m})$. The aforementioned design procedure leads to the following theoretical result.

Theorem 5.1:

With the thrust laws designed as (23) and (24), adaptive laws (29), (30), and (31), and the path parameter timing law (27), the quadrotor system described by (1) under Assumptions 2.1-2.6 will have the following results:

- i) The safety and performance requirements (8) and (12) will be met during formation.
- ii) The transformed tracking error $\eta_{\rm e}$ will converge into the set

$$\left\{ \eta_{\rm e} : |\eta_{\rm e}| < \varepsilon_{\eta}, \quad \varepsilon_{\eta} = \sqrt{\frac{2\varrho_1}{\kappa_1}} \right\}, \quad (34)$$

which implies that the LOS distance tracking error $d_{\rm e}$ will converge into the following region

$$\left\{ d_{\rm e} : \max(\varepsilon, 2\varepsilon + \varepsilon_{\chi_{\rm L}}) < d_{\rm e} < 2\varepsilon + \varepsilon_{\chi_{\rm H}} \right\}, \quad (35)$$

where $\varepsilon_{\chi_{\rm H}}$ and $\varepsilon_{\chi_{\rm L}}$ are given in (37) and (38) (see the next page), respectively.

- iii) The actual path speed \dot{s} will converge to a small neighburhood of its desired value $v_{\rm d}(s,d_{\rm a})$, i.e., $\lim\sup_{t\to\infty}|\dot{s}-v_{\rm d}(s,d_{\rm a})|=\varepsilon_{\eta}.$
- *iv*) The position control laws (23) and (24), adaptive laws (29), (30), and (31), and the path parameter timing law (27), are all uniformly bounded.

Proof:

Following (33), it can be concluded that $V_{\rm pos}$ is uniformly bounded, since from (33) we have

$$V_{\rm pos}(t) < \left(V_{\rm pos}(0) - \frac{\varrho_1}{\kappa_1}\right)e^{-\kappa_1 t} + \frac{\varrho_1}{\kappa_1}.$$
 (38)

The boundedness of $V_{\rm pos}$ implies boundedness of the "composite barrier function" (15), and hence $\eta_{\rm e}$ and $\eta_{\rm a}$ are both uniformly bounded. Hence, constraints requirements (8) and (12) are both satisfied. Moreover, we have $\limsup_{t\to\infty}V_{\rm pos}=\frac{\varrho_1}{\kappa_1}$, hence $\frac{1}{2}\eta_{\rm e}^2<\frac{\varrho_1}{\kappa_1}$ when $t\to\infty$, therefore $\eta_{\rm e}$ will converge to the set (34). Furthermore, uniform boundedness of $V_{\rm pos}$ implies boundedness of the adaptive estimates $\hat{\delta}_{\rm a}$, $\hat{w}_{\rm a}$, and $\hat{\mu}_m$, as well as boundedness of fictitious error z_v . Next, note that in the range that $-\varepsilon < d_{\rm e2} < \Omega_{\rm H2}$, $\eta_{\rm e}$ is a function in $d_{\rm e2}$, where recall that $d_{\rm e2} \triangleq d_{\rm e} - 2\varepsilon$. Hence, the range (12) gives the range for $d_{\rm e}$ given as in (35).

Furthermore, boundedness of $V_{\rm pos}$ implies boundedness of V_s , and hence $z_s=\dot{s}-v_{\rm d}$ is bounded. Given that the desired speed profile $v_{\rm d}$ is bounded, we can conclude that the actual path speed \dot{s} is also bounded. Moreover, since $\limsup_{t\to\infty}\frac{1}{2}z_s^2=\frac{\varrho_1}{\kappa_1}$, the speed assignment error will satisfy $|\dot{s}-v_{\rm d}(s,d_{\rm a})|<\varepsilon_\eta$ when $t\to\infty$.

Finally, given the boundedness of the adaptive estimates $\hat{\delta}_a$, \hat{w}_a , and $\hat{\mu}_m$, the path speed \dot{s} , as well as the fictitious error z_v , it can be checked that α_v and u are both uniformly bounded. Hence, it is clear to imply that the position control laws (23) and (24), adaptive laws (29), (30), and (31), and the path parameter timing law (27), are all uniformly bounded.

Remark 5.2:

In Theorem 5.1, using L'Hôpital's rule we can derive

$$\lim_{\varepsilon_{\eta} \to 0} \varepsilon_{\chi_{\rm H}} = 0, \quad \lim_{\varepsilon_{\eta} \to 0} \varepsilon_{\chi_{\rm L}} = 0.$$
 (39)

Hence, we can conclude from (35) that when the modified error variable $\eta_{\rm e}$ converges into a small neighborhood of zero, the actual LOS tracking errors $d_{\rm e}$ will also converge to a region arbitrarily close to 2ε , with $\varepsilon>0$ being an arbitrarily small constant.

B. Attitude Control Design and Results

Step 3:

Here we discuss the attitude kinematics of the quadrotor. Details can be seen in Appendix C (see (56)–(61)).

Step 4:

At this step, select the Lyapunov function candidate as $V_{\omega} = \frac{1}{2} z_{\omega}^{\mathrm{T}} M(\Theta) z_{\omega}$. With some algebraic analysis shown in Appendix D (see (62)–(63)), the torque law for the quadrotor is designed as

$$\tau = -\frac{\Psi(\Theta)z_{\omega} ||\bar{\tau}||^2 \hat{\rho}_J^2}{\sqrt{||\Psi(\Theta)z_{\omega}||^2 ||\bar{\tau}||^2 \hat{\rho}_J^2 + \epsilon^2}},$$
(40)

$$\bar{\tau} = K_{\omega} T^{\mathrm{T}}(\Theta) z_{\omega} + T^{\mathrm{T}}(\Theta) z_{\Theta} + \hat{\mu}_{J} \frac{T^{\mathrm{T}}(\Theta) z_{\omega} \Xi^{2}}{\sqrt{||z_{\omega}||^{2} \Xi^{2} + \epsilon^{2}}},$$
(41)

$$\varepsilon_{\chi_{\rm H}} = \frac{\left[\varepsilon_{\eta}(\Omega_{\rm H2} - \varepsilon) - \Omega_{\rm H2}\right] + \sqrt{\left[\varepsilon_{\eta}(\Omega_{\rm H2} - \varepsilon) - \Omega_{\rm H2}\right]^2 + 4\varepsilon_{\eta}^2 \Omega_{\rm H2} \varepsilon}}{2\varepsilon_{\eta}}$$
(37)

$$\varepsilon_{\chi_{L}} = \frac{\left[\varepsilon_{\eta}(\Omega_{H2} - \varepsilon) + \Omega_{H2}\right] - \sqrt{\left[\varepsilon_{\eta}(\Omega_{H2} - \varepsilon) + \Omega_{H2}\right]^{2} + 4\varepsilon_{\eta}^{2}\Omega_{H2}\varepsilon}}{2\varepsilon_{\eta}}$$
(38)

$$\dot{\hat{\rho}}_{J} = n_{\rho J} z_{\omega}^{\mathrm{T}} \Psi^{\mathrm{T}}(\Theta) \bar{\tau} - \sigma_{\rho J} \hat{\rho}_{J}, \tag{42}$$

$$\dot{\hat{\mu}}_{J} = n_{\mu J} \frac{||z_{\omega}||^{2} \Xi^{2}}{\sqrt{||z_{\omega}||^{2} \Xi^{2} + \epsilon^{2}}} - \sigma_{\mu J} \hat{\mu}_{J}, \tag{43}$$

where $\hat{\rho}_J(0) = \hat{\rho}_{J0}$ and $\hat{\mu}_J(0) = \hat{\mu}_{J0}$ are the initial conditions. $K_{\omega} > 0$ is a positive control gain. Ξ is introduced in (63). $\hat{\rho}_J$ is the adaptive estimate of the unknown constant $\rho_J = \frac{1}{I}$, and $\hat{\mu}_J$ is the adaptive estimate of the unknown constant $\bar{\mu}_J$ that is introduced in (63). $n_{\rho J}$, $\sigma_{\rho J}$, $n_{\mu J}$, and $\sigma_{\mu J}$ are positive design constants. Denote $V_{\text{att}} = V_{\Theta} + V_{\omega} + V_{\rho J} + V_{\mu J}, \ V_{\rho J} = \frac{J}{2n_{oJ}} \tilde{\rho}_J^2,$ $V_{\mu J} = \frac{1}{2n_{\mu J}} \tilde{\mu}_J^2$, where $\tilde{\rho}_J = \hat{\rho}_J - \rho_J$ and $\tilde{\mu}_J = \hat{\mu}_J - \bar{\mu}_J$. After some algebraic manipulation, we can arrive at

$$\dot{V}_{\text{att}} < -K_{\Theta} z_{\Theta}^{\text{T}} z_{\Theta} - K_{\omega} z_{\omega}^{\text{T}} z_{\omega} - \frac{\sigma_{\rho J} \underline{J}}{2n_{\rho J}} \tilde{\rho}_{J}^{2} - \frac{\sigma_{\mu J}}{2n_{\mu J}} \tilde{\mu}_{J}^{2} + \varrho_{2}, \tag{44}$$

where $\varrho_2 = \epsilon(\underline{J} + \bar{\mu}_J) + \frac{\sigma_{\rho J}}{2n_{\rho J}} \frac{1}{\underline{J}} + \frac{\sigma_{\mu J}}{2n_{uJ}} \bar{\mu}_J^2 + \frac{1}{2\nu} \bar{\Theta}_{\mathrm{d}}^2$. Hence,

$$\dot{V}_{\rm att} < -\kappa_2 V_{\rm att} + \varrho_2,\tag{45}$$

where $\kappa_2 \triangleq \min\left(2K_{\Theta}, \frac{2K_{\omega}}{\bar{M}}, \sigma_{\rho J}, \sigma_{\mu J}\right)$. The above design leads to the following result.

Theorem 5.2:

With the UAV torque laws as (40) and (41), and adaptive laws (42) and (43), the attitude control of the quadrotor system described by (2) and (3) under Assumptions 2.1– 2.6 has the following properties:

i) The attitude tracking error of the quadrotor z_{Θ} will converge into the set

$$\left\{ z_{\Theta} \mid ||z_{\Theta}|| < \varepsilon_{\eta}, \ \varepsilon_{\eta} = \sqrt{\frac{2\varrho_{2}}{\kappa_{2}}} \right\}, \tag{46}$$

ii) The torque laws (40) and (41), and adaptive laws (42) and (43) are all uniformly bounded.

Proof:

First of all, (45) leads to

$$V_{\rm att}(t) \le \left(V_{\rm att}(0) - \frac{\varrho_2}{\kappa_2}\right) e^{-\kappa_2 t} + \frac{\varrho_2}{\kappa_2},\tag{47}$$

hence $V_{\rm att}$ is uniformly bounded. Next, we have $\limsup_{t\to\infty}V_{\mathrm{att}}=\frac{\varrho_2}{\kappa_2}$, hence $\frac{1}{2}z_\Theta^2\leq\frac{\varrho_2}{\kappa_2}$ when $t\to\infty$, therefore z_Θ will converge to the set (46). Furthermore, boundedness of the adaptive estimates $\hat{\rho}_J$ and $\hat{\mu}_J$, as well as boundedness of the fictitious error z_{ω} , are now obvious since $V_{\rm att}$ is bounded. Therefore, it is straightforward to prove the boundedness of the torque laws (40) and (41), as well as adaptive laws (42) and (43).

The overall control algorithm can be summarized into the block diagram shown in Fig. 3.

VI. Simulation Studies

To demonstrate the effectiveness of the proposed attacker-resilient adaptive path following control scheme, a situation that an "attacker" attempts to collide with quadrotor on a certain part of the path is simulated. The model parameters of the quadrotor are m = 4 kg, $g = 9.81 \,\mathrm{m/s^2}$, and $J = \mathrm{diag}[0.109, 0.103, 0.0625] \,\mathrm{kg \cdot m^2}$. The "attacker" velocity is given as $v_a(Z_a)$ $0.3 + 0.25\sin(2d_a) + 0.25\cos(2d_a), 0.55 + 0.4\sin(2d_a) + 0.25\sin(2d_a)$ $0.45\cos(2d_{\rm a}), -1.25 - \frac{0.15}{d_{\rm a}+1}$]^T, which is dependent on relative distance from the quadrotor and unknown for the controller design. The desired path of the quadrotor can be described as $x_{\rm d}(s,d_{\rm a})=0.25s+\frac{0.85}{d_{\rm a}}+0.6,$ $y_{\rm d}(s,d_{\rm a})=3.5\sin(0.2s)+\frac{0.85}{d_{\rm a}}+0.6,$ and $z_{\rm d}(s,d_{\rm a})=-0.4s+\frac{1.15}{d_{\rm a}}+2.5.$ The desired speed assignment is selected as $v_{\rm d}(s,d_{\rm a})=1.5-e^{-0.5s}+\frac{2}{d_{\rm a}}$. The desired yaw angle ψ_d is chosen as $\psi_d = 0$. The safety constraint function is designed as $\Omega_{\rm a}(s) = 2 - e^{-0.1s}$. The performance constraint function is selected as $\Omega_{\rm H}(s,d_{\rm a})=7.1e^{-0.13s}-\frac{4.5}{d_{\rm a}}+1$ and the lower bound is $\varepsilon=0.05$. The external disturbances are $N_1(t)=$ $[0.05\cos(0.1t), \quad 0.05\cos(0.2t), \quad 0.15\cos(0.2t)]^{\mathrm{T}}$ and $N_2(t) = [0.02\cos(0.1t), 0.02\cos(0.2t), 0.15\cos(0.2t)]^{\mathrm{T}}.$

In this simulation, the number of neural network nodes is selected as n = 3 and the basis functions are given as $b_k(Z_a) = \exp \left[-\frac{(Z_a - \nu_k)^T (Z_a - \nu_k)}{c^2} \right], k = 1, 2, 3.$ For the basis functions, the width values are given as $\zeta_1 = \zeta_2 = \zeta_3 = 2$ and the receptive field's centers are selected as $\nu_1 = 0.5 \cdot \mathbf{1}_9$, $\nu_2 = \mathbf{1}_9$, and $\nu_3 = 1.5 \cdot \mathbf{1}_9$, where $\mathbf{1}_9 = [1, 1, 1, 1, 1, 1, 1, 1]^T \in \mathbb{R}^9$. We choose the design parameters as $n_{\delta a} = 0.45$, $n_{wa} = 0.35$, $n_{\mu m} = 0.35, n_{\rho J} = 0.25, n_{\mu J} = 0.35, \sigma_{\delta a} = 0.1,$ $\sigma_{wa} = 0.1, \ \sigma_{\mu m} = 0.1, \ \sigma_{\rho J} = 0.1, \ \sigma_{\mu J} = 0.1, \ \text{and}$ $\epsilon = 0.1$. The control gains are designed as $K_{\rm e} = 0.4$, $K_{\rm a} = 0.01, K_v = 0.7, K_s = 100, K_{\Theta} = 0.95,$ $\nu=0.5$, and $K_{\omega}=1.5$. The initial position of the quadrotor and "attacker" are $p(0) = [0, 0, 0]^T$ and $p_{\rm a}(0) = [1, -1, 10]^{\rm T}$, respectively. The initial attitude of the quadrotor is $\Theta(0) = [0, 0, 0.5]^{T}$. The initial translational and angular velocities of the quadrotor are zero.

For the potential function (PF)-based controller [24], controller gains are $\kappa_1 = 0.4$, $\kappa_2 = 1$, and $\kappa_{\rm obs} = 0.01$. The model parameters of the quadrotor and "attacker" dynamics are the same as we selected. Besides, initial states of the quadrotor and "attacker" are identical for both controllers.

The simulation results are presented in Figs. 4-10. The LOS attacker distance d_a under our proposed controller (M_1) and PF-based controller (M_2) [24] with the safety

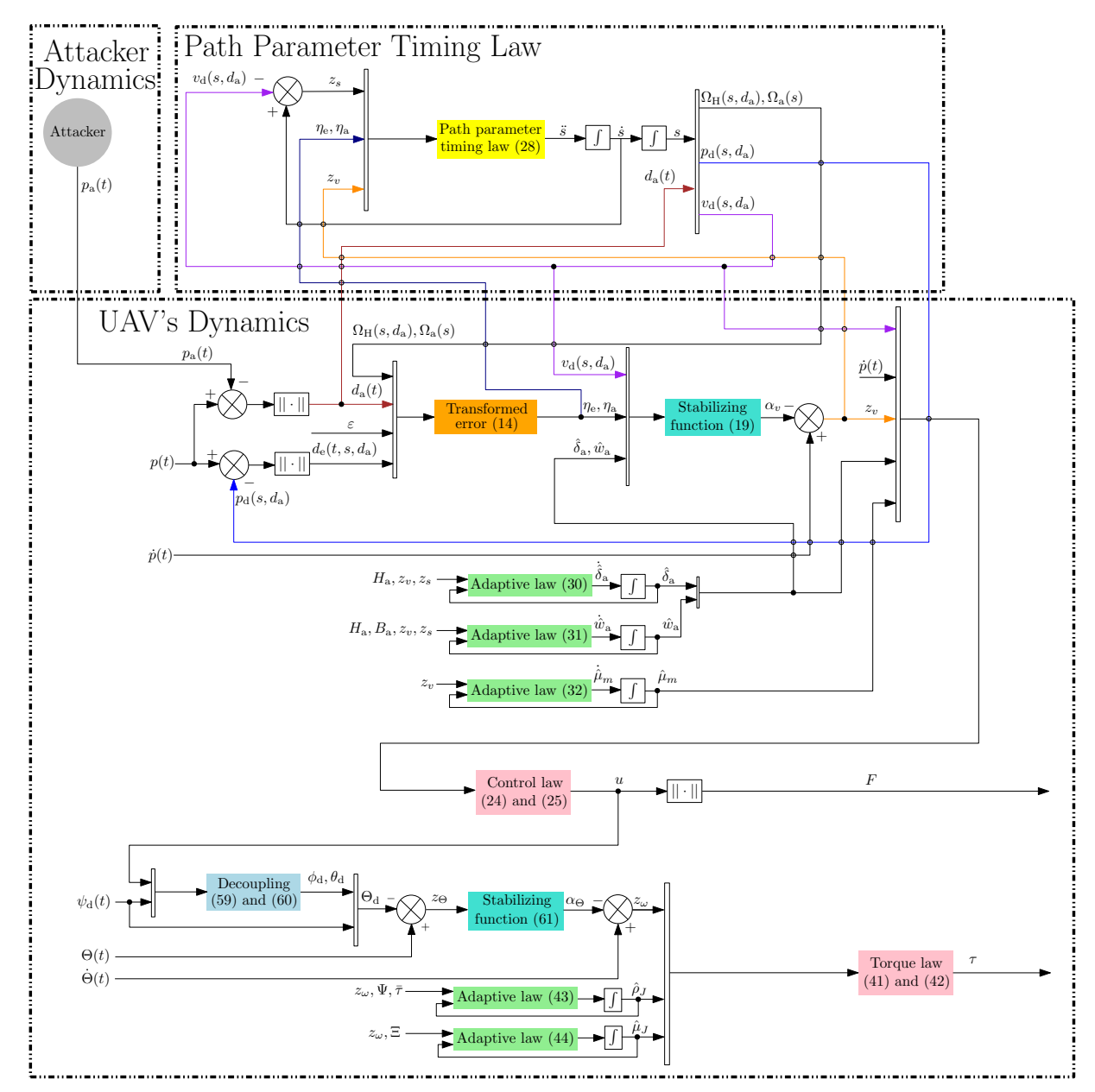


Fig. 3. Block diagram of the overall control algorithm.

constraint function $\Omega_{\rm a}$ are shown in Fig. 4. It can be seen that the LOS distance $d_{\rm a}$ never goes down to $\Omega_{\rm a}$, meaning that the safety constraint requirement (8) is always satisfied, which is not the case with the PF-based controller (M_2) . Therefore, under our proposed controller, the quadrotor is capable of collision avoidance with the "attacker". Note that the "attacker" is getting close to the quadrotor when $5 \leq t \leq 10$. During this period, we require that not only the desired path $p_{\rm d}$ is modified to stay far away the "attacker", but also the performance constraint function $\Omega_{\rm H}$ becomes more stringent to prevent the quadrotor from deviating much away from the desired path $p_{\rm d}$. Moreover, the desired path speed $v_{\rm d}$ should be able to increase, so that the quadrotor can quickly move away from the "attacker".

The 3D trajectories of the quadrotor and "attacker" are depicted in Fig. 5. It can be observed that the quadrotor can track its desired N-shaped path around two obstacles represented by cylinders without collision with the "attacker". The LOS distance tracking error $d_{\rm e}$ under our proposed controller is shown in Fig. 6 with the upper bound $\Omega_{\rm H}$ and the lower bound ε . From this figure, we see that $d_{\rm e}$ can converge to a small neighborhood of 2ε without any violation of the constraint requirements, where recall that ε can be an arbitrarily small positive constant. When $5 \le t \le 10$, the performance constraint function Ω_H decreases noticeably to make the quadrotor get close to its own desired path, which has been adjusted away from the "attacker". The profile of quadrotor attitudes, ϕ , θ , and ψ presented in Fig. 7 shows that the convergence of the attitudes to their own desired values

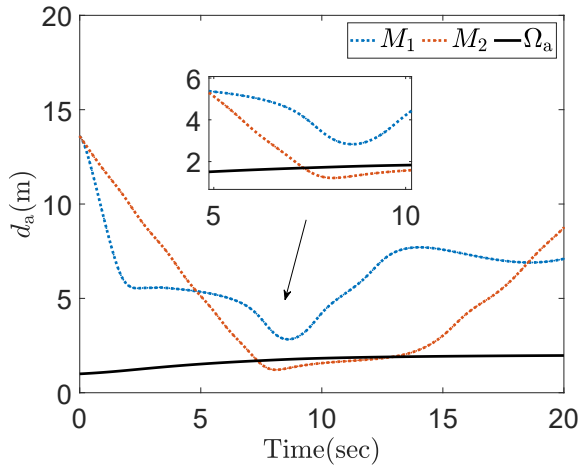


Fig. 4. Comparative simulation results of our proposed controller (M_1) and PF-based controller (M_2) in [24].

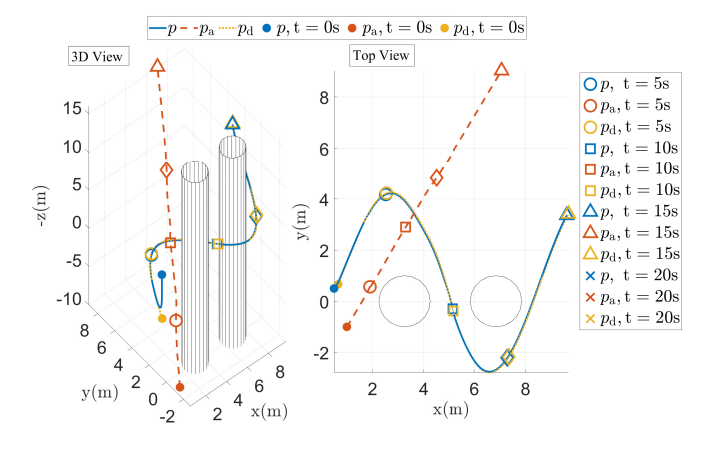


Fig. 5. Trajectories of the quadrotor and "attacker" in 3D space from a 3D perspective and a top-down view.

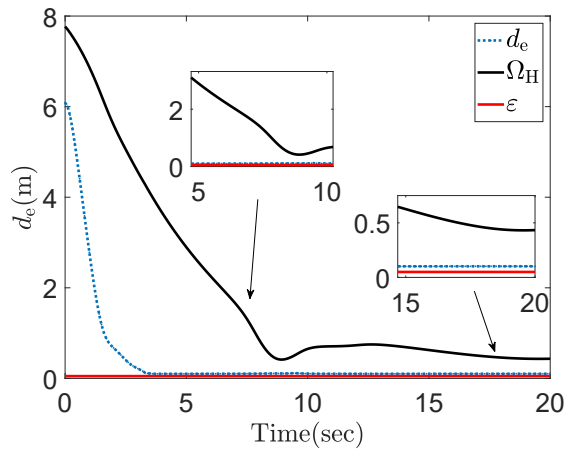


Fig. 6. The profile of the LOS distance tracking error $d_{\rm e}$ with $\Omega_{\rm H}$

despite lack of model parameters and the influence of external disturbances. The thrust F and torques τ_{ϕ} , τ_{θ} , and τ_{ψ} are plotted in Fig. 8 and Fig. 9, respectively. The thrust F can converge to a region close to the gravitational force of the quadrotor with unknown external disturbance N_1 . The torques can accommodate unknown disturbance N_2 despite the lack of accurate model parameters. The path speed \dot{s} and the desired speed assignment $v_{\rm d}$ are

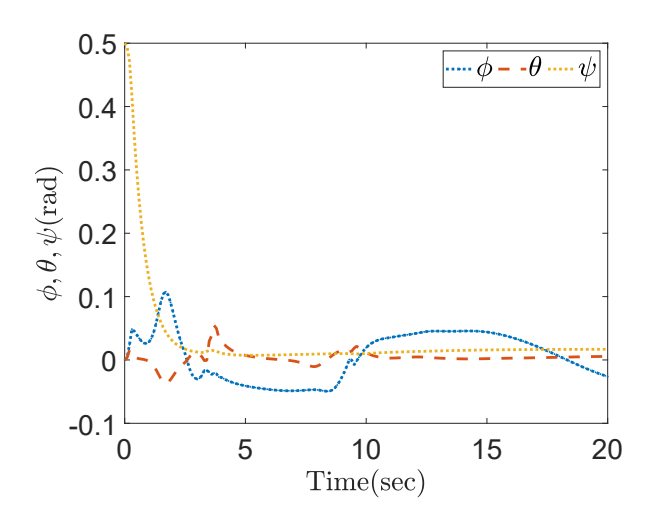


Fig. 7. The profile of quadrotor attitudes, ϕ , θ , and ψ .

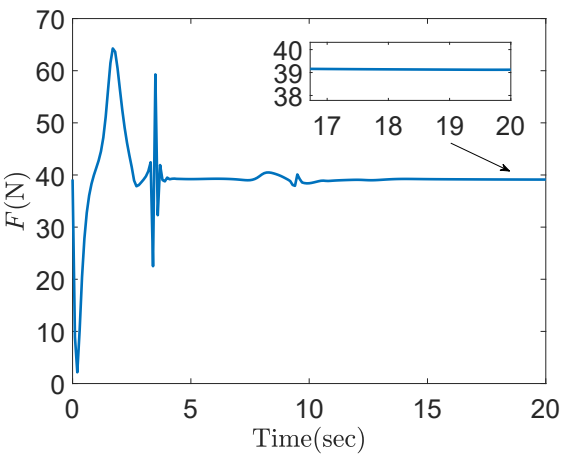


Fig. 8. The thrust F of the quadrotor.

exhibited in Fig. 10. It can be observed that the path speed \dot{s} can approach a neighborhood of the desired speed assignment $v_{\rm d}$. During $5 \leq t \leq 10$, when the "attacker" approaches the quadrotor, the desired speed assignment $v_{\rm d}$ can increase substantially, and \dot{s} is still able to track $v_{\rm d}$ quickly.

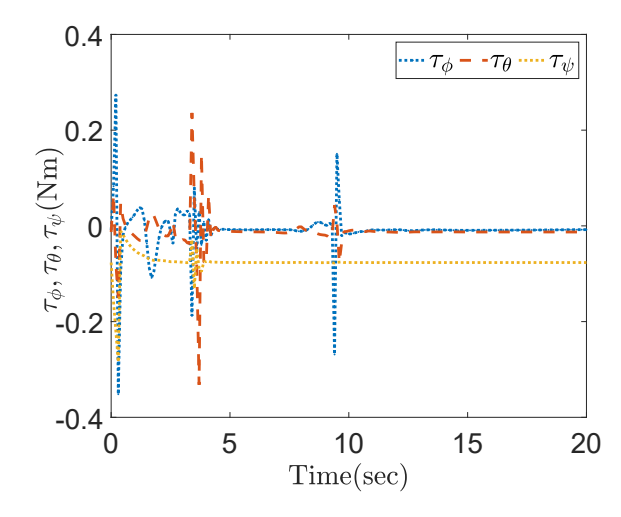


Fig. 9. Torques τ_{ϕ} , τ_{θ} , and τ_{ψ} of the quadrotor.

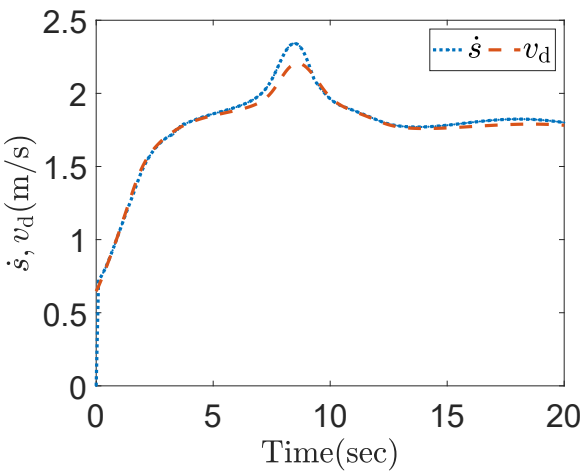


Fig. 10. The profile of the path speed \dot{s} and desired speed assignment $v_{\rm d}$.

Note that the sudden changes of attitudes ϕ , θ , and ψ , the thrust F, torques τ_{ϕ} , τ_{θ} , and τ_{ψ} , and the desired speed assignment $v_{\rm d}$ when $0 \le t \le 10$ are mainly caused by the "attacker" planning to approach and being near the quadrotor. Although the modification of $p_{\rm d}$, the magnification of $v_{\rm d}$, and the stringent adjustment of $\Omega_{\rm H}$ lead to these sudden and dramatic changes of closed-loop signals, the quadrotor can quickly get close to its desired path $p_{\rm d}$ adjusted away from the "attacker" such that performance and safety constraint requirements can be guaranteed. From the aforementioned discussion, we can now conclude that the simulation results confirm the theoretic analysis shown in Theorems 5.1 and 5.2.

VII. Conclusion

Instead of the conventional constant or time-varying constraint requirements, which are often conservative and cannot adapt to the dynamically changing environment, in this work we propose a new formulation of environmentaware dynamic constraints. More specifically, the desired path coordinate, desired path speed, and constraint requirements not only depend on a path parameter associated with the desired path, but also can adapt to the presence of an "attacker" nearby. In the context of quadrotor operations, a new adaptive path following architecture with a "composite barrier function" structure has been proposed to address both safety and performance constraints in a unified framework. Exponential convergence into small neighborhoods around the equilibrium for position and attitude tracking errors can be guaranteed. Future research directions include experiment verification of the proposed work, and addressing sensor/actuator uncertainties and noises.

Acknowledgment

The authors appreciate the Associate Editor and Reviewers from the IEEE Transactions on Aerospace and Electronic Systems for the helpful comments and constructive suggestions during the review process.

Appendix

A. System Dynamics

Denote
$$\Psi(\Theta)=T^{-1}(\Theta),$$
 from (2) we get
$$\omega=\Psi(\Theta)\dot{\Theta}. \tag{48}$$

Hence, multiply $J^{\rm T}$ on both sides of (3), and substitute (48) into (3), the angular motion dynamics of the UAV can be rewritten as

$$J^{\mathrm{T}}J\Big(\Psi(\Theta)\ddot{\Theta} + \dot{\Psi}(\Theta)\dot{\Theta}\Big) + J^{\mathrm{T}}\mathbb{S}\Big(\Psi(\Theta)\dot{\Theta}\Big)J\Psi(\Theta)\dot{\Theta} = J^{\mathrm{T}}\tau + J^{\mathrm{T}}N_{2}.$$
(49)

Now, multiply $\Psi^{\rm T}(\Theta)$ on both sides of (49), we can get

$$M(\Theta)\ddot{\Theta} + C(\Theta, \dot{\Theta})\dot{\Theta} = \Psi^{\mathrm{T}}(\Theta)J^{\mathrm{T}}\tau + \Psi^{\mathrm{T}}(\Theta)J^{\mathrm{T}}N_{2},$$
(50)

where

$$M(\Theta) = \Psi^{\mathrm{T}}(\Theta)J^{\mathrm{T}}J\Psi(\Theta),\tag{51}$$

$$C(\Theta, \dot{\Theta}) = \Psi^{\mathrm{T}}(\Theta) J^{\mathrm{T}} \mathbb{S} \Big(\Psi(\Theta) \dot{\Theta} \Big) J \Psi(\Theta)$$
$$+ \Psi^{\mathrm{T}}(\Theta) J^{\mathrm{T}} J \dot{\Psi}(\Theta), \tag{52}$$

where $M(\Theta)$ is symmetric and positive definite, and for any $x \in \mathbb{R}^3$, $x^{\mathrm{T}} \Big(\dot{M}(\Theta) - 2C(\Theta, \dot{\Theta}) \Big) x = 0$.

B. Step 2 of Backstepping Design

$$h_{s} = \frac{\partial \alpha_{v}}{\partial \Omega_{H2}} \frac{\partial \Omega_{H2}}{\partial s} + \frac{\partial \alpha_{v}}{\partial \Omega_{a}} \frac{d\Omega_{a}}{ds} + \frac{\partial \alpha_{v}}{\partial \left(\frac{\partial \Omega_{H2}}{\partial s}\right)} \frac{\partial^{2}\Omega_{H2}}{\partial s^{2}}$$

$$+ \frac{\partial \alpha_{v}}{\partial \left(\frac{d\Omega_{a}}{ds}\right)} \frac{d^{2}\Omega_{a}}{ds^{2}} + \frac{\partial \alpha_{v}}{\partial \left(\frac{\partial \Omega_{H2}}{\partial d_{a}}\right)} \frac{\partial^{2}\Omega_{H2}}{\partial d_{a}\partial s}$$

$$+ \frac{\partial \alpha_{v}}{\partial \left(\frac{\partial p_{d}}{\partial d_{a}}\right)} \frac{\partial^{2}p_{d}}{\partial d_{a}\partial s} + \frac{\partial \alpha_{v}}{\partial \left(\frac{\partial p_{d}}{\partial s}\right)} \frac{\partial^{2}p_{d}}{\partial s^{2}}$$

$$+ \frac{\partial \alpha_{v}}{\partial v_{d}} \frac{\partial v_{d}}{\partial s} - E_{\alpha d} \frac{\partial p_{d}}{\partial s},$$

$$(53)$$

$$H_{a} = \left(\frac{\partial \alpha_{v}}{\partial \Omega_{H2}} \frac{\partial \Omega_{H2}}{\partial d_{a}} + \frac{\partial \alpha_{v}}{\partial \left(\frac{\partial \Omega_{H2}}{\partial s}\right)} \frac{\partial^{2}\Omega_{H2}}{\partial s\partial d_{a}} \right)$$

$$+ \frac{\partial \alpha_{v}}{\partial \left(\frac{\partial \Omega_{H2}}{\partial d_{a}}\right)} \frac{\partial^{2}\Omega_{H2}}{\partial d_{a}^{2}} + \frac{\partial \alpha_{v}}{\partial \left(\frac{\partial p_{d}}{\partial d_{a}}\right)} \frac{\partial^{2}p_{d}}{\partial d_{a}^{2}}$$

$$+ \frac{\partial \alpha_{v}}{\partial \left(\frac{\partial \Omega_{H2}}{\partial s}\right)} \frac{\partial^{2}p_{d}}{\partial s\partial d_{a}} + \frac{\partial \alpha_{v}}{\partial v_{d}} \frac{\partial v_{d}}{\partial d_{a}} - E_{\alpha d} \frac{\partial p_{d}}{\partial d_{a}} \right) \frac{1}{d_{a}} E_{a}^{T}$$

$$+ \frac{\partial \alpha_{v}}{\partial \left(\frac{\partial p_{d}}{\partial s}\right)} \frac{\partial^{2}p_{d}}{\partial s\partial d_{a}} + \frac{\partial \alpha_{v}}{\partial v_{d}} \frac{\partial v_{d}}{\partial d_{a}} - E_{\alpha d} \frac{\partial p_{d}}{\partial d_{a}} \right) \frac{1}{d_{a}} E_{a}^{T}$$

$$+ \frac{\partial \alpha_{v}}{\partial \left(p - p_{a}\right)}$$

$$(54)$$

$$H_{p} = H_{a} + \frac{\partial \alpha_{v}}{\partial \left(p - p_{d}\right)}.$$

C. Step 3 of Backstepping Design

First, we need to extract the desired attitude from the control law $u=FR_{\rm d}e_z$, and we have

$$u = F \begin{bmatrix} c\phi_{d}s\theta_{d}c\psi_{d} + s\phi_{d}s\psi_{d} \\ c\phi_{d}s\theta_{d}s\psi_{d} - s\phi_{d}c\psi_{d} \\ c\phi_{d}c\theta_{d} \end{bmatrix},$$
 (56)

11

in which we recall that F is the thrust of the quadrotor. Here, for any designated reference yaw angle ψ_d satisfying Assumption 2.2, we define

$$F = ||u||, (57)$$

$$\phi_{\rm d} = \arcsin\left(\frac{u_1 \mathrm{s}\psi_{\rm d} - u_2 \mathrm{c}\psi_{\rm d}}{||u||}\right),$$
 (58)

$$\theta_{\rm d} = \arctan\left(\frac{u_1 c \psi_{\rm d} + u_2 s \psi_{\rm d}}{u_3}\right),$$
 (59)

where $u = [u_1, u_2, u_3]^T \in \mathbb{R}^3$.

Design the Lyapunov candidate as $V_{\Theta} = \frac{1}{2} z_{\Theta}^{\mathrm{T}} z_{\Theta}$, where z_{Θ} is the attitude tracking error defined in (13). Furthermore, define $z_{\omega} = \dot{\Theta} - \alpha_{\Theta}$, where α_{Θ} is a stabilizing function designed as

$$\alpha_{\Theta} = -\left(K_{\Theta} + \frac{\nu}{2}\right) z_{\Theta},\tag{60}$$

with K_{Θ} and ν being a positive control gain and a positive design constant, respectively. Taking derivative of $\phi_{\rm d}$ in (58) and $\theta_{\rm d}$ in (59) with respect to time yields $\dot{\phi}_{\rm d} = \frac{\partial \phi_{\rm d}}{\partial u_1} \dot{u}_1 + \frac{\partial \phi_{\rm d}}{\partial u_2} \dot{u}_2 + \frac{\partial \phi_{\rm d}}{\partial u_3} \dot{u}_3 + \frac{\partial \phi_{\rm d}}{\partial \psi_{\rm d}} \dot{\psi}_{\rm d}, \ \dot{\theta}_{\rm d} = \frac{\partial \theta_{\rm d}}{\partial u_1} \dot{u}_1 + \frac{\partial \theta_{\rm d}}{\partial u_2} \dot{u}_2 + \frac{\partial \theta_{\rm d}}{\partial \psi_{\rm d}} \dot{\psi}_{\rm d}, \ \text{where } u_1, \ u_2, \ u_3 \ \text{are bounded}$ according to Theorem 5.1, and $\psi_{\rm d}$ and $\dot{\psi}_{\rm d}$ are bounded according to Assumption 2.2, such that the terms $\frac{\partial \phi_{\rm d}}{\partial u_1}$, $\frac{\partial \phi_{\rm d}}{\partial u_2}$, $\frac{\partial \phi_{\rm d}}{\partial u_3}$, $\frac{\partial \phi_{\rm d}}{\partial \psi_{\rm d}}$, $\frac{\partial \theta_{\rm d}}{\partial u_1}$, $\frac{\partial \theta_{\rm d}}{\partial u_2}$, $\frac{\partial \theta_{\rm d}}{\partial u_3}$, and $\frac{\partial \theta_{\rm d}}{\partial \psi_{\rm d}}$ are all bounded. The result of differentiating u in (23) with respect to time can be combined with Theorem 5.1 to conclude the boundedness of \dot{u}_1 , \dot{u}_2 , and \dot{u}_3 . Therefore, $\dot{\Theta}_{\rm d}$ is bounded, which satisfies $||\dot{\Theta}_{\rm d}|| \leq \bar{\Theta}_{\rm d}$, where $\bar{\Theta}_{\rm d}$ is an unknown positive constant. Note that for any $\nu > 0$, $z_{\rm P}^{\rm T}\dot{\Theta}_{\rm d} \leq ||z_{\rm P}|| \bar{\Theta}_{\rm d} \leq \frac{1}{2\nu}\bar{\Theta}_{\rm d}^2 + \frac{\nu}{2}z_{\rm P}^{\rm T}z_{\rm P}$. Therefore

$$\dot{V}_{\Theta} \le \left(-K_{\Theta} z_{\Theta}^{\mathrm{T}} z_{\Theta} + z_{\Theta}^{\mathrm{T}} z_{\omega} + \frac{1}{2\nu} \bar{\Theta}_{\mathrm{d}}^{2} \right). \tag{61}$$

D. Step 4 of Backstepping Design

Taking derivative of V_{ω} yields

$$\dot{V}_{\omega} = z_{\omega}^{\mathrm{T}} \Big(\Psi^{\mathrm{T}}(\Theta) J^{\mathrm{T}}(\tau + N_2) - M(\Theta) \dot{\alpha}_{\Theta} - C(\Theta, \dot{\Theta}) \alpha_{\Theta} \Big), \tag{62}$$

where, for the term $z_{\omega}^{\mathrm{T}} \Big(\Psi^{\mathrm{T}}(\Theta) J^{\mathrm{T}} N_2 - M(\Theta) \dot{\alpha}_{\Theta} - C(\Theta, \dot{\Theta}) \alpha_{\Theta} \Big)$, we can get

$$z_{\omega}^{\mathrm{T}} \left(\Psi^{\mathrm{T}}(\Theta) J^{\mathrm{T}} N_{2} - M(\Theta) \dot{\alpha}_{\Theta} - C(\Theta, \dot{\Theta}) \alpha_{\Theta} \right)$$

$$= -z_{\omega}^{\mathrm{T}} \Psi^{\mathrm{T}}(\Theta) J^{\mathrm{T}} J \left(\Psi(\Theta) (-K_{\Theta} - \frac{\nu}{2}) (\dot{\Theta} - \dot{\Theta}_{\mathrm{d}}) + \dot{\Psi}(\Theta) \alpha_{\Theta} \right) - z_{\omega}^{\mathrm{T}} \Psi^{\mathrm{T}}(\Theta) J^{\mathrm{T}} \mathbb{S} (\Psi(\Theta) \dot{\Theta}) J \Psi(\Theta) \alpha_{\Theta}$$

$$+ z_{\omega}^{\mathrm{T}} \Psi^{\mathrm{T}}(\Theta) J^{\mathrm{T}} J J^{-1} N_{2}$$

$$\leq ||z_{\omega}|| ||\Psi(\Theta)|| ||J||^{2} \left(\left| \left| (K_{\Theta} + \frac{\nu}{2}) \Psi(\Theta) \dot{\Theta} \right| \right| + \left| \left| \dot{\Psi}(\Theta) \alpha_{\Theta} \right| \right| + \left| \left| \mathbb{S} (\Psi(\Theta) \dot{\Theta}) \right| \right| ||\Psi(\Theta) \alpha_{\Theta}||$$

$$+ \left| \dot{\Phi}_{\mathrm{d}} \right| \left| \left| (K_{\Theta} + \frac{\nu}{2}) \Psi(\Theta) \right| + \left| \left| J^{-1} N_{2} \right| \right| \right)$$

$$< \epsilon \bar{\mu}_{J} + \bar{\mu}_{J} \frac{||z_{\omega}||^{2} \Xi^{2}}{\sqrt{||z_{\omega}||^{2} \Xi^{2} + \epsilon^{2}}}, \tag{63}$$

where $\bar{\mu}_J$ is an unknown positive constant such that $||J||^2 (1 + \bar{\Theta}_d + ||J^{-1}N_2||) \leq \bar{\mu}_J$ and $\Xi \triangleq ||\Psi(\Theta)|| \left(\left| |\dot{\Psi}(\Theta)\alpha_\Theta|| + \left| \left| (K_\Theta + \frac{\nu}{2})\Psi(\Theta)\dot{\Theta}| \right| + \left| \left| |\mathbb{S}(\Psi(\Theta)\dot{\Theta})| \right| ||\Psi(\Theta)\alpha_\Theta|| + \left| \left| (K_\Theta + \frac{\nu}{2})\Psi(\Theta)| \right| + 1 \right) \right|$ is known.

REFERENCES

- D. Q. Mayne, J. B. Rawlings, C. V. Rao, and P. O. Scokaert, "Constrained model predictive control: stability and optimality," *Automatica*, vol. 36, no. 6, pp. 789–814, 2000.
- [2] S. L. de Oliveira Kothare and M. Morari, "Contractive model predictive control for constrained nonlinear systems," *IEEE Transactions on Automatic Control*, vol. 45, no. 6, pp. 1053–1071, 2000.
- [3] S. Mastellone, D. M. Stipanović, C. R. Graunke, K. A. Intlekofer, and M. W. Spong, "Formation control and collision avoidance for multi-agent non-holonomic systems: theory and experiments," *The International Journal of Robotics Research*, vol. 27, no. 1, pp. 107–126, 2008.
- [4] K. P. Tee, S. S. Ge, and E. H. Tay, "Barrier Lyapunov functions for the control of output-constrained nonlinear systems," *Automatica*, vol. 45, pp. 918–927, 2009.
- [5] X. Xu, P. Tabuada, J. W. Grizzle, and A. D. Ames, "Robustness of control barrier functions for safety critical control," *IFAC-PapersOnLine*, vol. 48, no. 27, pp. 54–61, 2015.
- [6] A. D. Ames, X. Xu, J. W. Grizzle, and P. Tabuada, "Control barrier function based quadratic programs for safety critical systems," *IEEE Transactions on Automatic Control*, vol. 62, no. 8, pp. 3861–3876, 2016.
- [7] C. P. Bechlioulis and G. A. Rovithakis, "Robust adaptive control of feedback linearizable MIMO nonlinear systems with prescribed performance," *IEEE Transactions on Automatic Control*, vol. 53, no. 9, pp. 2090–2099, 2008.
- [8] C. P. Bechlioulis and G. A. Rovithakis, "Robust partial-state feedback prescribed performance control of cascade systems with unknown nonlinearities," *IEEE Transactions on Automatic Control*, vol. 56, no. 9, pp. 2224–2230, 2011.
- [9] L. Lapierre, D. Soetanto, and A. Pascoal, "Nonlinear path following with applications to the control of autonomous underwater vehicles," in *Proc. IEEE International Conference on Decision and Control*, vol. 2, pp. 1256–1261, 2003.
- [10] A. P. Aguiar and J. P. Hespanha, "Trajectory-tracking and pathfollowing of underactuated autonomous vehicles with parametric modeling uncertainty," *IEEE Transactions on Automatic Control*, vol. 52, no. 8, pp. 1362–1379, 2007.
- [11] X. Xiang, L. Lapierre, C. Liu, and B. Jouvencel, "Path tracking: combined path following and trajectory tracking for autonomous underwater vehicles," in *Proc. IEEE/RSJ International Conference on Intelligent Robots and Systems*, pp. 3558–3563, 2011.
- [12] A. M. Lekkas and T. I. Fossen, "Line-of-sight guidance for path following of marine vehicles," *Advanced in Marine Robotics*, pp. 63–92, 2013.
- [13] T. I. Fossen, K. Y. Pettersen, and R. Galeazzi, "Line-of-sight path following for dubins paths with adaptive sideslip compensation of drift forces," *IEEE Transactions on Control Systems Tech*nology, vol. 23, no. 2, pp. 820–827, 2014.
- [14] X. Jin, S.-L. Dai, and J. Liang, "Fixed-time path-following control of an autonomous vehicle with path-dependent performance and feasibility constraints," *IEEE Transactions on Intelligent Vehicles*, 2021. accepted, to appear.
- [15] H. Zhu and J. Alonso-Mora, "Chance-constrained collision avoidance for MAVs in dynamic environments," *IEEE Robotics and Automation Letters*, vol. 4, no. 2, pp. 776–783, 2019.

- [16] K. Garg and D. Panagou, "Finite-time estimation and control for multi-aircraft systems under wind and dynamic obstacles," *Journal of Guidance, Control, and Dynamics*, vol. 42, no. 7, pp. 1489–1505, 2019.
- [17] V. S. Chipade and D. Panagou, "Herding an adversarial attacker to a safe area for defending safety-critical infrastructure," in *Proc.* American Control Conference, pp. 1035–1041, 2019.
- [18] J. Tordesillas and J. P. How, "Mader: trajectory planner in multiagent and dynamic environments," *IEEE Transactions on Robotics*, vol. 38, no. 1, pp. 463–476, 2021.
- [19] J. Qi, J. Guo, M. Wang, C. Wu, and Z. Ma, "Formation tracking and obstacle avoidance for multiple quadrotors with static and dynamic obstacles," *IEEE Robotics and Automation Letters*, vol. 7, no. 2, pp. 1713–1720, 2022.
- [20] S. X. Wei, A. Dixit, S. Tomar, and J. W. Burdick, "Moving obstacle avoidance: a data-driven risk-aware approach," *IEEE Control Systems Letters*, 2022. accepted, to appear.
- [21] V. P. Tran, M. A. Garratt, K. Kasmarik, and S. G. Anavatti, "Dynamic frontier-led swarming: Multi-robot repeated coverage in dynamic environments," *IEEE/CAA Journal of Automatica Sinica*, vol. 10, no. 3, pp. 646–661, 2023.
- [22] R. E. Allen and M. Pavone, "A real-time framework for kinodynamic planning in dynamic environments with application to quadrotor obstacle avoidance," *Robotics and Autonomous Systems*, vol. 115, pp. 174–193, 2019.
- [23] P. Fiorini and Z. Shiller, "Motion planning in dynamic environments using velocity obstacles," *The International Journal of Robotics Research*, vol. 17, no. 7, pp. 760–772, 1998.
- [24] M. C. P. Santos, C. D. Rosales, M. Sarcinelli-Filho, and R. Carelli, "A novel null-space-based UAV trajectory tracking controller with collision avoidance," *IEEE/ASME Transactions on Mecha*tronics, vol. 22, no. 6, pp. 2543–2553, 2017.
- [25] H. Wang, Y. Li, W. Yu, J. He, and X. Guan, "Moving obstacle avoidance and topology recovery for multi-agent systems," in Proc. American Control Conference, pp. 2696–2701, 2019.
- [26] B. Lindqvist, S. S. Mansouri, A.-a. Agha-mohammadi, and G. Nikolakopoulos, "Nonlinear MPC for collision avoidance and control of UAVs with dynamic obstacles," *IEEE robotics* and automation letters, vol. 5, no. 4, pp. 6001–6008, 2020.
- [27] M. Braquet and E. Bakolas, "Vector field-based collision avoidance for moving obstacles with time-varying elliptical shape," arXiv preprint arXiv:2207.01747, 2022.
- [28] B. Wang, Y. Zhang, and W. Zhang, "Integrated path planning and trajectory tracking control for quadrotor uavs with obstacle avoidance in the presence of environmental and systematic uncertainties: Theory and experiment," *Aerospace Science and Technology*, vol. 120, p. 107277, 2022.
- [29] T. Nägeli, J. Alonso-Mora, A. Domahidi, D. Rus, and O. Hilliges, "Real-time motion planning for aerial videography with dynamic obstacle avoidance and viewpoint optimization," *IEEE Robotics and Automation Letters*, vol. 2, no. 3, pp. 1696–1703, 2017.
- [30] G. Chen, P. Peng, P. Zhang, and W. Dong, "Risk-aware trajectory sampling for quadrotor obstacle avoidance in dynamic environments," *IEEE Transactions on Industrial Electronics*, vol. 70, no. 12, pp. 12606–12615, 2023.
- [31] X. Jin, "Fault tolerant finite-time leader-follower formation control for autonomous surface vessels with los range and angle constraints," *Automatica*, vol. 68, pp. 228–236, 2016.
- [32] X. Jin, "Nonrepetitive leader-follower formation tracking for multiagent systems with LOS range and angle constraints using iterative learning control," *IEEE Transactions on Cybernetics*, vol. 49, no. 5, pp. 1748–1758, 2018.
- [33] S.-L. Dai, S. He, X. Chen, and X. Jin, "Adaptive leader-follower formation control of nonholonomic mobile robots with prescribed transient and steady-state performance," *IEEE Trans*actions on Industrial Informatics. accepted, to appear.

- [34] X. Jin, S.-L. Dai, J. Liang, and D. Guo, "Multirobot system formation control with multiple performance and feasibility constraints," *IEEE Transactions on Control Systems Technology*, 2021.
 accepted, to appear.
- [35] X. Jin, S.-L. Dai, and J. Liang, "Adaptive constrained formation tracking control for a tractor-trailer mobile robot team with multiple constraints," *IEEE Transactions on Automatic Control*, 2022. accepted, to appear.
- [36] X. Jin and Z. Hu, "Adaptive cooperative load transportation by a team of quadrotors with multiple constraint requirements," *IEEE Transactions on Intelligent Transportation Systems*, 2022. accepted, to appear.
- [37] W. Xie, W. Zhang, and C. Silvestre, "Saturated backstepping-based tracking control of a quadrotor with uncertain vehicle parameters and external disturbances," *IEEE Control Systems Letters*, vol. 6, pp. 1634–1639, 2022.
- [38] Z. Zuo and C. Wang, "Adaptive trajectory tracking control of output constrained multi-rotors systems," *IET Control Theory & Applications*, vol. 8, no. 13, pp. 1163–1174, 2014.
- [39] C. Wang and Y. Lin, "Decentralized adaptive tracking control for a class of interconnected nonlinear time-varying systems," *Automatica*, vol. 54, pp. 16–24, 2015.
- [40] D. Bernstein, "Matrix mathematics: theory, facts, and formulas," Princeton University Press, 2003.
- [41] A. G. Bors and I. Pitas, "Median radial basis function neural network," *IEEE Transactions on Neural Networks*, vol. 7, no. 6, pp. 1351–1364, 1996.
- [42] H. Simon, "Neural networks: a comprehensive foundation," Prentice Hall, 1999.
- [43] R. J. Schilling, J. J. Carroll, and A. F. Al-Ajlouni, "Approximation of nonlinear systems with radial basis function neural networks," *IEEE Transactions on Neural Networks*, vol. 12, no. 1, pp. 1– 15, 2001.



Xu Jin (S'12–M'19) received the Bachelor of Engineering (BEng) degree in electrical and computer engineering (First Hons.) from the National University of Singapore, Singapore, the Master of Applied Science (MASc) degree in electrical and computer engineering from the University of Toronto, Toronto, ON, Canada, the Master of Science (MS) degree in mathematics from the Georgia Institute of Technology, Atlanta, GA, USA, and the Doctor

of Philosophy (PhD) degree in aerospace engineering from the Georgia Institute of Technology, Atlanta, GA, USA.

Dr. Jin is currently an Assistant Professor with the Department of Mechanical and Aerospace Engineering, University of Kentucky, Lexington, KY, USA. His current research interests include adaptive and iterative learning control with applications to intelligent vehicles, autonomous robots, and nonlinear multiagent systems.



Zhongjun Hu received the B.Eng. degree in automation from the college of information engineering, Zhejiang University of Technology, Hangzhou, China, in 2018, and the master of science degree in electrical and computer engineering from the Ohio State University, Columbus, OH, USA, in 2020. He is currently working toward a Ph.D. with the Department of Mechanical and Aerospace Engineering, University of Kentucky, Lexington, KY, USA.

His research interests include adaptive control and its application of multi-agent systems.

13